



ADVANCED REVIEW

Visualizing stem cells in vivo using magnetic resonance imaging

Shehzahdi Shebbrin Moonshi¹  | Yuao Wu¹  | Hang Thu Ta^{1,2,3} 

¹Queensland Microtechnology and Nanotechnology Centre, Griffith University, Nathan, Queensland, Australia

²Australian Institute for Bioengineering and Nanotechnology, University of Queensland, St Lucia, Queensland, Australia

³School of Environment and Science, Griffith University, Nathan, Queensland, Australia

Correspondence

Hang Thu Ta, Queensland Microtechnology and Nanotechnology Centre, Griffith University, Nathan, Queensland 4111, Australia.
Email: h.ta@griffith.edu.au

Funding information

National Health and Medical Research Council, Grant/Award Numbers: APP1037310, APP1182347, APP2002827; National Heart Foundation of Australia, Grant/Award Number: 102761

Edited by: Julian Vastl, Associate Editor and Gregory Lanza, Co-Editor-in-Chief

Abstract

Stem cell (SC) therapies displayed encouraging efficacy and clinical outcome in various disorders. Despite this huge hype, clinical translation of SC therapy has been disheartening due to contradictory results from clinical trials. The ability to monitor migration and engraftment of cells in vivo represents an ideal strategy in cell therapy. Therefore, suitable imaging approach to track MSCs would allow understanding of migratory and homing efficiency, optimal route of delivery and engraftment of cells at targeted location. Hence, longitudinal tracking of SCs is crucial for the optimization of treatment parameters, leading to improved clinical outcome and translation. Magnetic resonance imaging (MRI) represents a suitable imaging modality to observe cells non-invasively and repeatedly. Tracking is achieved when cells are incubated prior to implantation with appropriate contrast agents (CA) or tracers which can then be detected in an MRI scan. This review explores and emphasizes the importance of monitoring the distribution and fate of SCs post-implantation using current contrast agents, such as positive CAs including paramagnetic metals (gadolinium), negative contrast agents such as superparamagnetic iron oxides and ¹⁹F containing tracers, specifically for the in vivo tracking of MSCs using MRI.

This article is categorized under:

Diagnostic Tools > In Vivo Nanodiagnostics and Imaging
Nanotechnology Approaches to Biology > Nanoscale Systems in Biology
Therapeutic Approaches and Drug Discovery > Emerging Technologies

KEYWORDS

¹⁹F tracers, cell tracking, contrast agents, longitudinal, magnetic resonance imaging (MRI), mesenchymal, stem cells, superparamagnetic iron oxides (SPIO)

1 | INTRODUCTION

Mesenchymal stem cells (MSCs) have generated massive attention for its application as a bioactive agent or delivery tool to target and treat many disease conditions (Y. Wang et al., 2013). Reports of the therapeutic employment of MSCs from the clinical trials database (<http://clinicaltrials.gov>) revealed 1002 registered studies, with 307 completed trials and 145 trials that have progressed to phase 2 of clinical trials.

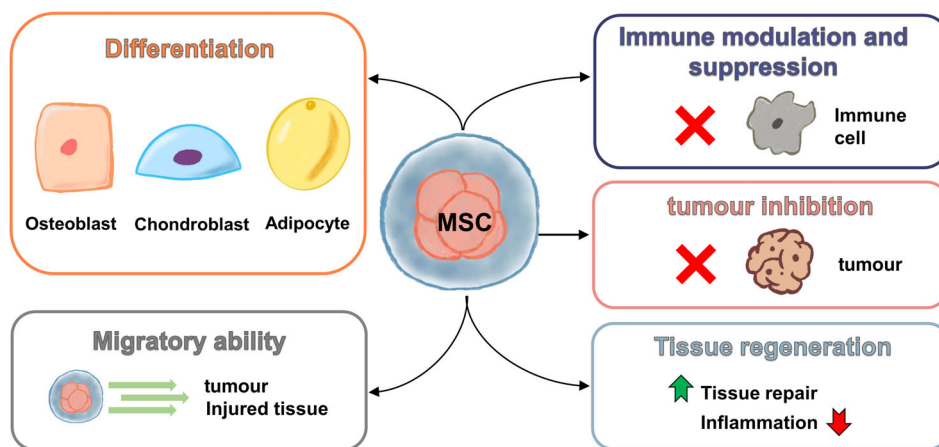


FIGURE 1 A schematic diagram representing the biological properties of MSCs that are correlated with their therapeutic effects

MSC is a popular treatment choice in various diseases because of its efficacy in immunomodulation and immunosuppression (Chen et al., 2011), differentiation (S. Wang et al., 2012), intrinsic migratory affinity to diseased tissues or tumor microenvironments (Danielyan et al., 2020), and anti-cancer efficacy in specific tumor types (Figure 1) (Chien et al., 2011). While MSC therapy has demonstrated promising potential, outcomes from studies are usually inconsistent, hence hindering the progress of MSC therapy to the clinic (Srinivas, Aarntzen, et al., 2010). In a recent clinical publication, it is clearly highlighted that the optimal parameters such as injected dose and infusion interval of SCs are limited till date and no clear optimized treatment protocol has been established (Yang et al., 2021). Moreover, MSC treatment can only be effective when viable cells move toward targeted location and engraft after injection (Hmadcha et al., 2020). Inconsistent data obtained from clinical trial studies is partially due to the absence of strategy to track the distribution and accumulation of injected cells upon implantation in subjects (Rosenzweig, 2006).

In vivo tracking of cells represents an apt approach for the surveillance of the biodistribution and fate of injected cells in subjects. Hence, it is critical to develop precise and reliable imaging approach to monitor the movement of cells to optimize treatment parameters for enhanced therapy efficacy (Janjic & Ahrens, 2009). Accordingly, in vivo monitoring of cells via imaging strategies must be exploited to establish effective treatment parameters including number of cells required, frequency and timing of injections, route of administration, and homing efficiency to target sites to ensure optimal treatment efficacy. Therefore, this review emphasizes the importance of in vivo tracking of SCs post-implantation using current contrast agents or fluorinated tracers employed for tracking using MRI. MRI imaging agents that have been utilized specifically for SCs tracking have been discussed in this review and can be classified into the following categories: positive contrast agents containing paramagnetic metals (gadolinium), negative contrast agents comprising of superparamagnetic iron oxides (SPIO), and non-proton agents (fluorine). Our review highlights the specific characteristics including advantages and limitations corresponding to SC tracking of these MR imaging techniques. Notably, our review focuses on the in vivo tracking of SCs specifically, potential directions in SC tracking, challenges for clinical translation, and recent developments in this field. The most recent review on a similar topic was 3 years ago by Bulte and Daldrup-Link, which discussed the in vivo tracking of cell therapies in general utilizing MRI, SPECT, and PET imaging (Bulte & Daldrup-Link, 2018). Another similar review by Srivastava and Bulte discussed various techniques to stem cell labeling and tracking using different imaging modalities such as MRI, SPECT and PET (Srivastava & Bulte, 2014). However, this review was published almost 7 years ago. Therefore, our review provides an updated and more focused discussion on the in vivo tracking of stem cells, particularly using MRI and its recent preclinical and clinical developments.

2 | IN VIVO CELL TRACKING TECHNIQUES BASED ON MRI

Cellular imaging involves non-invasive and repeated tracking of the cells of interest (Bulte & Kraitchman, 2004). Magnetic resonance imaging (MRI), positron emission tomography (PET), computed tomography (CT), single-photon emission computed tomography (SPECT), ultrasound (US), and fluorescence and bioluminescence imaging (BLI) are

imaging modalities employed for in vivo cell tracking. Each technique is accompanied with several advantages and limitations (Table 1; Bernsen et al., 2015).

Overall, cells must be labeled before implantation to allow visualization and tracking in imaging studies. Fluorescence and BLI are commonly used techniques to track MSCs in small animals due to their ease of use (A. Taylor et al., 2018). However, due to the limitation of signal dispersion in deeper tissue, this technique cannot be employed in larger animals or clinically (Sutton et al., 2008). Ultrasound is widely available and involves simple application. Nonetheless, difficulty to reach many anatomical sites accompanied with low spatial resolution prevents accurate tracking of cells. Furthermore, techniques involving intracellular US contrast are not yet established in comparison to other cell tracking modalities.

In the clinic, Indium-111 (^{111}In)-oxine is the only FDA approved agent for radionuclide tracking of leucocytes (de Vries et al., 2005). However, clinical application of radionuclide tracking of cells longitudinally are hampered by short half-life (2–3 h) of radioisotopes, limited retention in cells, radiotoxicity, and safety issues in patients, hence their dosage and recurrent usage are strictly controlled (Srivastava & Bulte, 2014). Moreover, radionuclide techniques must also be combined with other imaging modality, such as CT, to provide anatomical imaging, resulting in increased cost and complexity (Aarntzen et al., 2013). While PET imaging provides detection of labeled cells with exceptional sensitivity and tissue penetration, it has low spatial resolution, short term signal acquisition and exposure to radiation (Aarntzen et al., 2013).

MRI is a medical imaging technique that allows repetitive tracking of cells in comparison to other imaging techniques (Boehm-Sturm et al., 2011). MRI is generally used for soft tissue imaging and does not involve radiation, hence is considered safe and suitable for repeated imaging at high resolution (E. T. Ahrens & Bulte, 2013). Typically, cells are labeled before implantation with an agent that is visible in an MRI scan (Srinivas, Heerschap, et al., 2010). MRI signal can be generated or controlled in various methods including with positive contrast agents containing paramagnetic metals (gadolinium), negative contrast agents comprising of superparamagnetic iron oxides (SPIO) and ^{19}F containing tracers which will be discussed in this review (Table 2).

Cells can be directly labeled after co-incubation with contrast agents or with the assistance of transfection agents or electroporation. After which, cells are collected and washed before being administered into the subject. Then MRI scan is acquired to visualize cells in the subject (Figure 2). MRI contrast agents that have been employed to label cells are discussed below.

2.1 | Metal ion-based MRI contrast agents

2.1.1 | Positive contrast agents

Previously, positive contrast agents for cell tracking have been developed in various forms, including liposomal and micellar nanoparticles, carbon nanostructures, and polymer coated Gadolinium (Gd)-oxide particles (Aspord et al., 2013; Tran et al., 2014; Tseng et al., 2010). Gadolinium (Gd^{3+}) and Manganese (Mn^{2+}) metal ions are generally classified as T_1 contrast agents (Geng et al., 2015). The main advantage for MR image analysis involving tracking of SCs is attained via positive contrast T_1 agents as opposed to negative contrast (T_2 agents), which can be ambiguous to interpret (Yu Liu et al., 2011). Moreover, upon cell death, the low molecular weight Gd can avoid macrophage phagocytosis

TABLE 1 Advantages and drawbacks of various imaging modalities for the in vivo tracking of stem cells

	MRI	PET	SPECT	US	FLI	BLI
Tissue penetration depth	High	High	High	Moderate	Low	Low
Sensitivity of cell detection	High	Moderate	Moderate	Moderate	Moderate	Moderate
Spatial resolution	High	Low	Low	Moderate	Low	Low
Ability to monitor cells longitudinally	Yes	Yes	No	No	Yes	Yes
Clinical application in cell tracking	Yes	Yes	Yes	No	No	No
Exposure to radiation	No	Yes	Yes	No	No	No

Abbreviations: BLI, bioluminescence imaging; FLI, fluorescence imaging; MRI, magnetic resonance imaging; PET, positron emission tomography; SPECT, single-photon emission computed tomography; US, ultrasound.

TABLE 2 The various magnetic resonance imaging contrast agents available

MRI agent	MRI technique	MRI contrast	Quantification of cell number	Minimum number of cells detected	Clinical trial	Advantages	Limitations
Gadolinium	T ₁ -weighted ¹ H MRI	Positive	Indirect quantification	10 ² (Aspord et al., 2013; Figueiredo et al., 2013)	None	More specific than T ₂ agents.	Less sensitive and lower cell detection limit than T ₂ agents.
Manganese agent	T ₁ -weighted ¹ H MRI	Positive	Indirect quantification	10 ³ (T. Kim et al., 2011; Sterenczak et al., 2012)	None	More specific than T ₂ agents.	Long term cytotoxic effects are unknown.
SPIO/USPIO agent	T ₂ -weighted ¹ H MRI	Negative	Indirect quantification	Single cell detection possible (Shapiro et al., 2006; Zhang et al., 2005)	Phase 1 trial completed (NCT03651791) using USPIO labeled MSCs in heart disease. This study identified the iron-oxide labeled MSCs after 26 weeks.	High sensitivity. Single cell detection possible.	Indirect quantification of cell number. Not specific. Contrast generated by SPIO labeled cells can be confused with other sources.
Chemical exchange saturation transfer (CEST) reporter agents	¹ H CEST MRI	Differential contrast	Indirect quantification	10 ⁴ (Ferrauto et al., 2013)	None	Ability to detect multiple cell populations in the same location. Ability to turn contrast on and off. Reduced adverse effects.	Similar to T ₁ agents, lower sensitivity than T ₂ agents.
Fluorinated tracer	¹⁹ F MRI	Hot spot	Direct quantification	10 ³ –10 ⁵ (Moonshi et al., 2018)	Phase 1 trial (NCT02921373) is not yet recruiting for the tracking of Celsense labeled PBMC.	Specific, unequivocal and quantitative strategy of tracking labeled cells.	Sensitivity to detect small cell numbers is potentially lower.

hence evading false positive signal and generating highly specific contrast (Geng et al., 2015). Nonetheless, T₁ agents are less sensitive and have a lower cell detection limit than T₂ agents.

Various studies have demonstrated *in vivo* tracking of SCs using a Gd-based contrast agent (Klasson et al., 2008; Michel Modo et al., 2002; Sitharaman et al., 2007). Guenoun et al. demonstrated tracking of MSCs with Gd-liposomes in rat models in a 3 T MR scanner (Guenoun et al., 2012). MSCs were detected for at least 2 weeks post-implantation of labeled cells and Gd-liposomes had no significant consequence on the viability, proliferation and differentiation abilities of MSCs (Guenoun et al., 2012). Other studies demonstrated successful tracking of MSCs labeled with Gd-DTPA in a rat ischemic model in a 7 T MR scanner (Geng et al., 2015). Gd contrast agent had negligible adverse effects on the phenotypical characteristics and viability of cells (Geng et al., 2015). Importantly, MSCs were observed 1 week after injection of labeled cells (Geng et al., 2015).

Clinical translation of Gd-based contrast agent has been hindered due to the ambiguity involved in the long-term cytotoxicity effects of the contrast agent despite minimal or no adverse effects reported on the phenotypical and

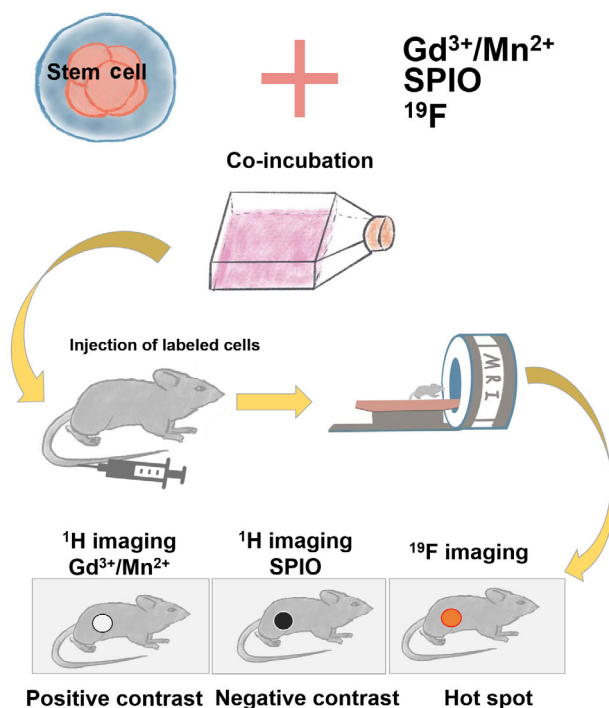


FIGURE 2 Schematic showing prior labeling of cells with magnetic resonance nanoparticle contrast agents. Cells are labeled ex vivo by co-incubation of contrast agents directly into cell culture media. MRI scan acquired detects cells in the subject. Cells labeled with positive contrast agents produce a hyperintense signal, while cells labeled with negative contrast agents produce a hypointense signal. Cells labeled with fluorinated nanoparticles are detected as “hot spot” in MR images

functional characteristics of SCs (M. Modo et al., 2009). Brekke et al. discovered that Gd-based contrast agents increased reactive oxygen species (ROS) and decreased proliferation in neural stem cells (NSCs) (Brekke et al., 2007). Hence, this study concluded that Gd-based contrast agent might have an adverse consequence on the regenerative and typical function of NSCs (Brekke et al., 2007). Additionally, Gd-based contrast agent has been associated to cause progressive fibrosis development in multiple organs in patients with renal failure (M. Modo et al., 2009). Until now, no current study involving MRI tracking of SC tracking solely with Gd-based contrast agents has been published with the most recent study published 6 years ago in 2015 (Geng et al., 2015).

2.1.2 | Negative contrast agents containing superparamagnetic iron oxides

Iron oxide-based nanomaterials have been employed widely for imaging of various disease conditions (Arndt et al., 2020; Gaston et al., 2018; Yajun Liu et al., 2019; Rehman et al., 2021; H. Ta et al., 2010; H. T. Ta et al., 2018; Vazquez-Prada et al., 2020; Wu, Vazquez-Prada, et al., 2021; Wu, Zhang, et al., 2021; Yusof et al., 2019; Zia et al., 2020). In SC tracking studies using MRI, T_2/T_2^* contrast is the most commonly employed strategy (Frangioni & Hajjar, 2004). Areas where SPIO particles accumulate appear hypointense or dark on images (Figure 2). Ultra-small superparamagnetic iron oxides (USPIO) particles are more commonly utilized in comparison to SPIO as smaller particles are internalized more proficiently in SCs and has a higher bioavailability, hence making it more suitable for the tracking of SCs for an extended period of time (Song et al., 2007).

Nonetheless, both SPIO or USPIO contrast agents are employed for SC labeling as these agents generate a strong negative contrast or hypointensity distinctively in T_2/T_2^* weighted MR images (Bulte & Kraitchman, 2004). Importantly, this technique is extremely sensitive whereby even single labeled cells have been tracked in vivo under specific conditions (Duyn, 2013; Heyn et al., 2006). Notably, iron oxide is safe, eco-friendly and is phagocytosed by stellate macrophages in liver, where the iron is acquired and released by cells for iron metabolism via biochemical pathways (Parivar et al., 2016). However, ROS generation via the Fenton and Haber–Weiss reactions on the surfaces of IONPs, can lead to damaging effects in cells, tissues, and organs (Wydra et al., 2015). While it has been established that single

cells can be detected and this feature provides immense advantage for monitoring SC biodistribution (Shapiro et al., 2006), hypointense regions generated from the accumulation of SPIO labeled cells can be mistaken with other factors such as bleeding (Park et al., 2015). Contrast produced in MRI images due to SPIO labeled SCs can be analogous to blood, bone fragments, air, or susceptibility artifacts arising from surgical procedures (Park et al., 2015). Therefore, monitoring and explicit identification of labeled cells will be extremely difficult due to the similarity of contrast effects in cases of traumatic injury with the presence of hemorrhage, which may complicate image interpretation (Kwon et al., 2015; Moelker et al., 2006). Labeled cells are quantified indirectly through the measurement of “number of black pixels” or the “signal void volume” and it is established by a difference corresponding to pre-implantation imaging time point (M. Modo et al., 2009). Besides, quantification of the number of cells *in vivo* is questionable as signal loss produced by SPIO labeled cells are achieved indirectly (M. Modo et al., 2009). Therefore, tracking of SCs distribution via this technique can be ambiguous as quantification is based on indirect contrast acquired. Similarly, monitoring and quantification of SCs through positive contrast agents can be equivocal.

Two clinically approved SPIO agents are ferumoxides (Feridex, USA and Endorem, Europe), with a particle size range between 120 and 180 nm, and ferucarbotran (Resovist), with a particle size of 60 nm (Y.-X. J. Wang, 2015). Ferumoxides and Resovist are only permitted specifically for liver imaging (Y.-X. J. Wang, 2015). Hence, these agents are not approved by FDA for the purpose of SPIO SC labeling considering its effect on the function and phenotype of SCs has not been entirely established (Y. X. J. Wang et al., 2008). Preclinical studies encompassing the *in vivo* tracking of SCs using SPIONs have been reported in various animal models (Table 3; Bull et al., 2014). Jing et al. demonstrated tracking of MSCs in the cartilage of a rabbit model using Feridex-protamine sulfate complex as the SPION (Jing et al., 2008). Results from this study established that the SPION did not modify inherent MSCs characteristics, and T_2 hypointense signals were detected for at least 12 weeks after initial implantation of labeled cells (Jing et al., 2008). Another study with Feridex has verified the feasibility of labeling SCs with SPIO nanoparticles accompanied with the employment of commercially available transfection agents (Frank et al., 2003). However, clinical translation of these techniques is complicated because SPIO labeling with transfection agents involves safety issues (de Vries et al., 2005). Accordingly, both Feridex and Resovist are no longer produced and commercially available (Y.-X. J. Wang, 2015).

Novel dextran coated SPIONs to track BM-MSCs have been employed in a myocardial infarcted animal model to ascertain SCs efficacy in cardiac tissue regeneration (Chapon et al., 2009). Results from this study confirmed that the SPION labeled MSCs could be monitored for up to 6 weeks after initial implantation of cells. While no improved ventricular function was detected, this study highlighted the capability of tracking cells with dextran coated SPIONs (Chapon et al., 2009). There have not been many studies published in the past 5 years despite numerous reports on the successful *in vivo* tracking of SCs labeled with SPIONs. Studies involving longitudinal tracking of SCs labeled with IONPs using MRI in the past 6 years are compiled in Table 3.

Therefore, there is an unmet requirement for the development of SPIO contrast agents that is efficient and reliable in tracking SC distribution after implantation without changing inherent therapeutic and phenotypical attributes of cells.

2.2 | ^{19}F MRI

MRI is a suitable imaging technique to monitor movement of SCs upon injection in subjects. As discussed previously in the Section 2.1.2, signal loss (hypointense areas) generated due to SPIO labeled cells can be ambiguous as quantification is dependent on indirect contrast (Kwon et al., 2015). An alternative strategy to overcome these limitations is via the employment of ^{19}F MRI, which involves the utilization of tracking cells labeled with fluorinated tracers to clearly differentiate cells from other background (Boehm-Sturm et al., 2011).

^{19}F MRI delivers high specificity, explicitly detecting signal from fluorinated tracer as there is negligible ^{19}F signal from the body (Tirota et al., 2015). ^{19}F MRI combines a “hot spot” to the MR effect which is then overlaid on the conventional anatomical ^1H image (Tirota et al., 2015). Conveniently, both ^{19}F MR and ^1H MR images are acquired concurrently using the same imaging modality problems. ^{19}F hot spot imaging has clear advantage in comparison to PET or SPECT as it does not involve radiation hence allowing serial imaging of subjects over time (Ruiz-Cabello et al., 2008). As ^{19}F MRI only detects signal from fluorinated tracers due to the lack of background signal in the body, signal acquired is specific to labeled cells unlike metal ion-based cell labeling methodologies where false positive cell detection is highly possible (Eric T. Ahrens et al., 2005). Besides, the signal acquired is directly proportional to the amount of ^{19}F present (Eric T. Ahrens et al., 2005). Notably, quantification of cell numbers from the MR imaging is possible when the average ^{19}F content per cell is known (Srinivas et al., 2012). Consequently, the high specificity which

TABLE 3 An analysis of magnetic nanoparticles for longitudinal stem cell tracking in animal models using magnetic resonance imaging in the past 6 years

Type of nanoparticle and labeling parameters	Disease model	MRI strength	Clinical outcome	References
Dextran based polymer coated SPION 6 mL of 25 µg/mL of SPION for 2×10^6 cells	Controlled cortical impact injury	7 T	Labeled cells were observed longitudinally at injured site till 14 days after intranasal injection.	Shahrer et al. (2019)
FeraTrack 1 mL of (20–25 µg/mL) of SPION for 1.0×10^6 cells 21.97 ± 5.23 pg (iron/cell)	Mouse amyotrophic lateral sclerosis Rat model of optic-nerve crush. C6 glioma bearing nude mice	7 T 7 T 3 T	Labeled cells were observed longitudinally till 34 days after symptomatic injection. Labeled cells were detected for up to 18 weeks after intravitreal injection. Labeled cells homing to the tumors were detected up to 10 days post-injection.	Gubert et al. (2016) Mesentier-Louro et al. (2014) S. J. Kim et al. (2016)
Bionized nanoferrite (BNF) nanoparticles and gadolinium-diethylenetriaminepentaacetate (GdDTPA) were used as SPIONs and gadolinium chelates 1 mL of 600 µg of iron/mL for 2.5×10^6 cells 14.8 ± 1.7 pg (iron/cell)	Mouse brain injury model	9.4 T	Labeled cells detected via T ₁ and T ₂ imaging longitudinally for up to 1-week post-injection.	Ngen et al. (2015)
Dextran based polymer coated SPION 1 mL of 10 µg/mL of SPION for 1×10^5 cells	Rat heart infarction model	9.4 T	Labeled cells detected for up to 6 weeks after injection at lesioned site. Improved ventricular function was not observed in the rats.	Chapon et al. (2009)
Iron oxide loaded biodegradable poly(lactide-co-glycolide) microparticles 1 mL of 137 µg/mL of IONP for 1×10^5 cells 3–50 pg (iron/cell)	Healthy mouse model	7 T	In vivo monitoring of cell migration in rat brains over 2 weeks.	Granot et al. (2014)
Molday ION Rhodamine B (MIRB) and Resovist MIRB: 1 mL of 100 µg/mL for 0.09×10^5 cells Resovist: 1 mL of 50 µg/mL for 0.09×10^5 cells	Healthy rat model	7 T	Labeled cells were detected for up to 14 days after intracerebral transplantation. Viability and differentiation of cells were only affected at higher NP concentrations.	Ohki et al. (2020)

allows quantification of cell numbers through ¹⁹F MRI is highly advantageous for the optimization of SC treatment efficacy. Overall, ¹⁹F MRI delivers a highly specific, explicit, and quantitative strategy for visualizing cells in vivo.

Nonetheless, in comparison to SPIO agents, the sensitivity of ¹⁹F labeling to detect small cell numbers is potentially lower (Srinivas, Heerschap, et al., 2010). Even so, as ¹⁹F atom is absent from the body the background and the signal-to-noise ratio (SNR) of the ¹⁹F images will be considerably lower in comparison to ¹H MRI, permitting unequivocal cell detection devoid of false positives (Eric T. Ahrens et al., 2005). Therefore, ¹⁹F MRI is particularly suitable for the tracking of SCs therapy especially in disease models associated with traumatic injury and hemorrhage.

Recently, studies have focused on the development of ¹⁹F MRI agents such as ¹⁹F containing small molecules, ¹⁹F containing macromolecules and perfluorocarbon (PFC) emulsions, with PFCs being the most commonly used tracers (Janjic & Ahrens, 2009; Knight et al., 2011; Yu, 2013).

TABLE 4 Summary of longitudinal studies of in vivo tracking of ^{19}F labeled stem cells

^{19}F tracer	Type of cells	MRI strength	MRI-sequence/ acquisition time	Fluorine content/cell	Days imaged post-implantation	Length of time ^{19}F signal detected	Animal model	References
Partially fluorinated polymers (PFPs) 1 mL of 10 mg/mL (PFPs) in 5×10^5 cells	Human PMSCs	9.4 T	RARE sequence (12 min)	$2.6 \pm 0.1 \times 10^{12}$ ^{19}F atoms/cell Injected 1×10^6 labeled cells	0, 1 h, 24 h, 7	7 days	Healthy NOD SCID mice	Moonshi et al. (2018)
Celsense 1 mL of 6 mg/mL (Celsense) in 1×10^5 cells	hBM-MSCs	9.4 T	balanced steady-state free precession 3D (bSSFP) (1 h)	$7.1 \pm 1.7 \times 10^{10}$ ^{19}F atoms/cell Injected 1.5×10^6 labeled cells	0, 3, 12, 17, 26	26 days	Healthy nude mice	Ribot et al. (2014)
PFCE 8 μL of 4.8 mM final PFCE concentration for 5.0×10^6 cells	Mouse NSCs	9.4 T	Fast Spin Echo	4.8 mM PFCE Injected 4×10^4 labeled cells	3, 7, 14	2 weeks	Healthy nude mice	Ruiz-Cabello et al. (2008)
Celsense 1 mL of 12 mg/mL (Celsense) in 1×10^5 cells	hNSCs	11.7 T	Turbo Spin echo (1.5 h)	$3.70 \pm 0.78 \times 10^{12}$ ^{19}F atoms/cell Injected 1.5×10^5 labeled cells	2, 6	6 days	Healthy nude mice	Boehm-Sturm et al. (2011)
Celsense 1 mL of 5 mg/mL (Celsense) in 5×10^5 cells	hNSCs	7 T	Fast Spin Echo (45 min)	1.96×10^{12} ^{19}F atoms/cell Injected 2.1– 2.5×10^6 labeled cells	0, 1, 7	7 days	Rat stroke model	Bible et al. (2012)
Celsense 1 mL of 2.5 mg/mL (Celsense) in 2×10^5 cells	hMSCs	9.4 T	3D bSSFP <60 min	8.2×10^{10} to 2.4×10^{11} ^{19}F atoms/cell Injected 1×10^6 labeled cells	0, 2, 6, 10, 14	14 days	Healthy mice	Gaudet et al. (2017)

PFPE has been validated to be an ideal ^{19}F imaging agent with its simple synthesis and ^{19}F NMR spectrum (Gerhardt & Lagow, 1978). Many reported cell labeling studies have engaged the use of PFC emulsions (~100–300 nm) because of their high ^{19}F content (Table 4; Bible et al., 2012; Boehm-Sturm et al., 2011; Gaudet et al., 2015; Ribot et al., 2014). Nevertheless, a huge apprehension with nanoemulsion is the development of larger particles at the expense of the smaller particles due to the inevitable progression of Ostwald ripening (P. Taylor, 1998). Hence, in comparison to emulsions, the main advantage of smaller labels such as partially fluorinated polymers is that they can be manipulated based on the strategic aim of the studies. Few studies have reported MR visualization of ^{19}F labeled SCs in vivo (Table 4; Bible et al., 2012; Boehm-Sturm et al., 2011; Gaudet et al., 2015; Ribot et al., 2014). Out of these studies, only five groups have performed longitudinal imaging to track the fate of SCs after implantation (Table 4; Bible et al., 2012; Boehm-Sturm et al., 2014; Gaudet et al., 2015; Ribot et al., 2014; Ruiz-Cabello et al., 2008).

Interestingly, these imaging studies were conducted in SCs labeled with commercial PFCs nanoemulsion (Celsense Inc., Pittsburg, Pennsylvania) and its implantation into a healthy mouse model (Boehm-Sturm et al., 2011; Gaudet et al., 2015; Ribot et al., 2014). Data obtained from these researches established a longitudinal detection and

quantification of labeled cells for up to 14 days with no significant deleterious outcomes on SCs characteristics (Boehm-Sturm et al., 2011; Ruiz-Cabello et al., 2008). Nonetheless, efficacy and feasibility of tracers to monitor labeled SCs must also be performed in diseased models as SCs might behave differently in a diseased microenvironment in comparison to a healthy model.

Besides, tracking of SCs in a healthy model is not clinically relatable as SCs are mainly employed as a therapeutic agent in diseased models. Hence, it is vital to ascertain MRI tracking ability in diseased models. Only one study by Boehm-Sturm et al. compared MRI ^{19}F signal acquired from Celsense labeled SCs injected in naïve and stroke mice and interestingly reported no significant difference between both mice models (Figure 3a; Boehm-Sturm et al., 2014). Furthermore, MRI ^{19}F signal persisted for 4 weeks post-implantation of labeled SCs in both healthy and diseased model (Boehm-Sturm et al., 2014). Hence, in the future, preclinical MRI studies involving tracking of SCs should explore the feasibility of tracers and its application in disease models for a more clinically relatable outcome. Another study reported both 3D-bSSFP MRI of ^{19}F and ^1H signal from Celsense-labeled and Molday ION Rhodamine B (MIRB)-labeled hMSC, respectively, were visualized at corresponding implantation location for almost 4 weeks post-implantation of cells (Figure 3b(C-F)) (Ribot et al., 2014). Nonetheless, it should be highlighted that a signal loss

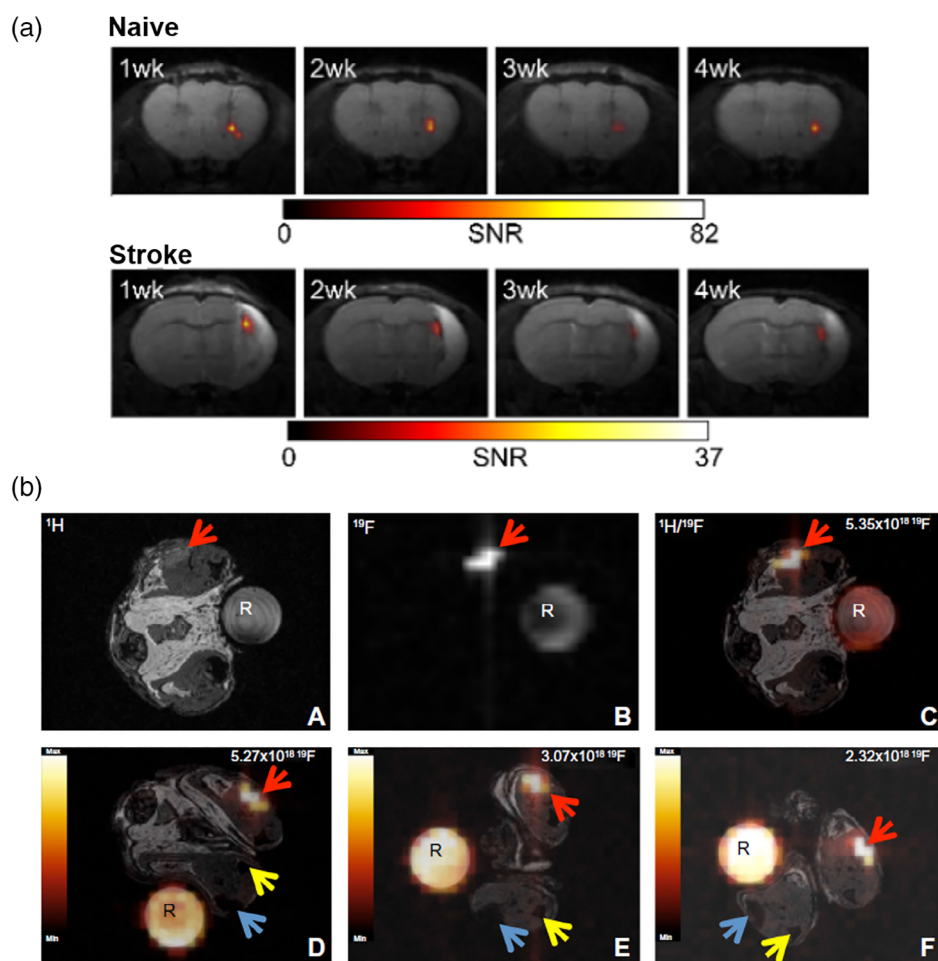


FIGURE 3 Longitudinal tracking of fluorinated labeled SCs in mice model. (a) ^{19}F imaging performed 1–4 weeks after implantation of labeled SCs into naive mice and stroke animals that underwent middle cerebral arterial occlusion 48 h before (Boehm-Sturm et al., 2014). (b) Representative axial ^1H image (A), ^{19}F image (B), and overlay (C) of ^{19}F image on ^1H anatomical image with the ^{19}F rendered in “hot-iron” color scale on the day of the cell injection. Axial images of the same mouse imaged 3 days (D), 12 days (E), and 26 days (F) after the injection. The red and blue arrows point to the Celsense-labeled mesenchymal stem cells (MSCs) and Molday ION rhodamine B (MIRB)-labeled hMSC injection sites, respectively. The yellow arrows point to bone. “R” designates the fluorine reference tube. The number of fluorine atoms quantified for the cell sense-labeled MSCs injection sites at each time point are indicated at the top right of each image. The minimum/maximum intensities for the hot iron scale represent values of 10,058/610,470 (D), 10,910/381,030 (E), and 17,335/413,250 (F) (Ribot et al., 2014)

(depicted by yellow arrows) was also displayed by the bones of mouse legs. Hence, this false positive signal acquired from mouse bones emphasizes ambiguity involved in tracking of iron labeled cells which was also discussed in earlier part of this review (Ribot et al., 2014). In the past couple of years, ^{19}F MRI in vivo tracking also involves utilization of immune cells labeled with Celsense (Chapelin et al., 2017, 2018; Kennis et al., 2019).

Fluorinated block copolymers have been proposed as an alternative to PFCs as an ^{19}F MRI agent (Peng et al., 2009). Polymeric agents have inherent advantages as imaging tracers for MRI as they are easily manipulated, with the option to attach functional groups, which permits the inclusion of multiple imaging modalities, bioactive treatments and targeting ligands for a more focused and precise imaging in subjects (Thurecht, 2012). Moonshi et al developed partially fluorinated polymers with a fluorine content of ~ 21.4 wt%, with PFPE as the fluorine constituent and oligo(ethylene glycol) methyl ether methacrylate (OEGMA) as the hydrophilic component (Moonshi et al., 2018). Importantly, they demonstrated that labeled MSCs were observed for 1 week in a mouse model within a short MRI acquisition time of 12 min (Moonshi et al., 2018). Notably, partially fluorinated polymers (PFPs) employed in this study for MRI tracking had no substantial harmful consequence on the viability, differentiation abilities, and expression of specific MSC markers (Moonshi et al., 2018). ^{19}F MRI has not been employed routinely in the clinic despite reported successful studies demonstrating in vivo tracking of cells, predominantly due to the lack of efficient and reliable tracers. Therefore, further emphasis and efforts must be directed to the development of innovative ^{19}F tracers for the progress toward the clinical application of ^{19}F MRI.

3 | CONCERNS AND LIMITATIONS

Cell division which leads to dilution of intracellular agents imposes a challenge for long-term in vivo SC tracking, irrespective of the type of MR tracer or contrast agent. Moreover, a limitation of most nanoparticle-based imaging tracers includes the lack of ability to discriminate between live and dead cells. Cell death can cause diffusion of tracers eventually leads to a loss of MRI detectability (Bulte & Daldrup-Link, 2018). Moreover, cell death can effect in the possible transfer of the imaging agent to neighboring macrophages and may result in false positive signals if a large population accumulate in an area of interest (Srinivas et al., 2007). Even though this was observed in a few studies (Srinivas et al., 2007), most in vivo research displayed the opposite whereby tracked cells of interest displayed in MRI are not macrophages (Srinivas et al., 2007). Hence, apprehension of macrophage ingestion of labeled cells seems overstated and should not dampen future prospects of research in this area.

Several parameters such as size, surface charge, coating, and routes of administration of MR contrast agents have substantial impact on the safety profile and clearance of these NPs (Arami et al., 2015). In general, liver and spleen which forms part of mononuclear phagocytic system plays a major role in the clearance of i.v. injected IONPs and PFC nanoemulsions (Arami et al., 2015; Jacoby et al., 2014). Nonetheless, upon injection of high iron concentration, surplus IONPs gets transported to other macrophage rich organs such as lungs for elimination from the circulatory system (Levy et al., 2011). A recent clinical study conducted in patients with chronic ischemic heart disease confirmed that intramyocardial injection of USPIO labeled MSC did not have an adverse effect on these patients 6 months post-treatment (Mathiasen et al., 2019). While there are growing research assessing the clearance mechanism and toxicity of MR contrast agents, data obtained are not consistent due to the variation in NPs characteristics and experimental parameters utilized in different studies (Feng et al., 2018).

PFCs have been established as a safe and biocompatible compound accompanied with no substantial reported adverse effects (Krafft, 2001). Additionally, they are exploited in various biomedical applications including its role in the preparation of synthetic blood (Clark, 1966; Geyer, 1973). PFCs are removed from the body through exhalation and bowel excretion (Castro et al., 1984). Consequently, there are many reported studies on the biocompatibility, biodistribution and clearance mechanism of PFCs, presenting these polymers as ideal candidates as a suitable MRI tracer (Geyer, 1973). Nonetheless, ^{19}F MRI studies involving tracking of SCs labeled with PFC nanoemulsion in mouse model demonstrated label retention despite the death of implanted cells (Bible et al., 2012; Boehm-Sturm et al., 2014). In this case, prolonged retention of cell tracer is also not ideal as it does not reflect the true viability of cell treatment and can result in toxicity issues that can develop from the slow clearance of tracer. Also, PEGylated NPs covertly avoid Kupffer cells in the liver allowing these NPs to gain longer circulation time and selectively taken up by spleen macrophages (Cole et al., 2011). Although longer circulation time of MR contrast agents is ideal for longitudinal tracking purpose, long term toxicity of these agents must be further evaluated (Levy et al., 2011).

Interestingly, all ^{19}F imaging studies till date involving the tracking of SCs have injected labeled cells subcutaneously or in a localized microenvironment to ascertain feasibility of tracers (Table 4). Moreover, these studies did not progress to evaluate biodistribution of labeled cells after implantation via other clinically relevant methods such as i.v., so on. While it is crucial to understand feasibility of tracers in a subcutaneous model as a preliminary assessment, further studies must be conducted to understand the true efficacy of fluorinated agents as a MR cell imaging tracer.

Feridex has been reported to influence chondrogenic differentiation potential but not adipogenic or osteogenic differentiation in MSCs (Kostura et al., 2004). Therefore, it is crucial that MRI cell tracers have negligible impact on critical inherent SCs characteristics such as differentiation potential, phenotypical and expected therapeutic function as any alterations after labeling could have an adverse consequence on the reliability and efficacy of the MSC therapy. Consequently, any type of MRI agents developed for the purpose of SC tracking must be thoroughly and rigorously evaluated in correspondence to the criteria validated for MSCs by the International Society for Cellular Therapy (ISCT).

4 | OTHER POTENTIAL DIRECTIONS IN STEM CELL TRACKING

As described earlier in this review, while several studies have established successful longitudinal MRI tracking of MSCs labeled with T_1 -shortening Gd-based contrast agents, clinical translation of this contrast agent has been impeded due to the equivocality involved in the long-term safety of these agents (Geng et al., 2015; M. Modo et al., 2009). Consequently, there is an unmet clinical need for a suitable alternative T_1 -shortening contrast agent that can replace Gd-based contrast agents (Bales et al., 2019; Besenhard et al., 2021). Preferentially, these alternative agents should have the same T_1 -shortening effect accompanied with a substantial reduction in accumulated toxicity in comparison to Gd-based contrast agents. Interestingly, Boehm-Sturm et al. have studied the ability of chelates loaded with paramagnetic ferric iron (Fe^{3+}) in lieu of paramagnetic gadolinium (Gd^{3+}) for T_1 -weighted dynamic contrast-enhanced imaging in in vivo breast cancer model (Boehm-Sturm et al., 2017). Their results indicated that, upon intravenous injection, these low molecular weight iron chelates displayed comparable contrast effects and enhancement kinetics to commercially available Gd-DTPA (Magnevist; Bayer, Leverkusen, Germany) with a 1.5-T MRI (Boehm-Sturm et al., 2017).

Also, a recent study in 2020 demonstrated the utilization of iron (III)-quercetin complex as a T_1 -positive contrast agent for the potential monitoring of cells in vivo (Papan et al., 2020). Interestingly, this group established that the T_1 relaxivity value of their iron complex in both water (range of $1.5\text{--}4.2\text{ mM}^{-1}\text{ s}^{-1}$) and plasma (range of $3.4\text{--}6.6\text{ mM}^{-1}\text{ s}^{-1}$) measured at 1.5 T was comparable to other clinical T_1 -positive contrast agents such as Gd-DTPA and Gd-DOTA. Also, this study displayed enhancement of T_1 signal intensity in vitro accompanied with negligible adverse effects in labeled peripheral blood mononuclear cells (Papan et al., 2020). While SPION based T_2 contrast agents encompasses several advantages including biocompatibility and high sensitivity, contrast produced by SPIO labeled cells can be confused with other factors such as bleeding or blood vessels, hence hindering clear monitoring of cells (Park et al., 2015). Therefore, employing the use of iron instead of Gd chelates as an alternative hypercontrast imaging agent delivers a promising strategy that can allow the tracking of labeled SCs while obviating toxicity involved with Gd and ambiguity correlated with SPION based T_2 contrast agents. Subsequently, further research efforts need to be channeled in this direction to provide a long-term safety profile of iron chelates as a T_1 -contrast agent for the successful serial tracking of labeled stem cells in vivo.

While MR contrast imaging agents such as SPIONs and fluorinated tracers have been established to successfully monitor cell distribution over time, a crucial limitation of all NP based agents is the inability to distinguish between live and dead cells (Bulte & Daldrup-Link, 2018). Hence, it is unclear if a stem cell treatment fails due to cell death upon transplantation or poor survival of therapeutic cells (Hmadcha et al., 2020). Hence, a non-invasive MR imaging technique that can track and ascertain viability of cells could expedite clinical translation of cell therapies.

Reporter gene labeling confers an advantage as the reporter gene is transfected into the DNA of the therapeutic cells and protein expression can only be generated by viable cells and is passed on to daughter cells (Eric T. Ahrens et al., 2014; Li et al., 2018). MRI is then employed with the utilization of a specific probe to non-invasively monitor transgene expression of viable cells in vivo (Li et al., 2018). Hence, MR imaging of reporter gene expression allows the tracking of cell survival and proliferation after implantation. Overall, MRI reporter genes can be classified into three main categories including reporter genes that can attain chemical exchange saturation transfer (CEST), reporter enzymes, and iron homeostasis protein (Jurgielewicz et al., 2017). A detailed description of MRI reporter genes in stem cell tracking is presented by review articles from Jurgielewicz and Vande Velde et al. (Jurgielewicz et al., 2017; Vande Velde et al., 2013).

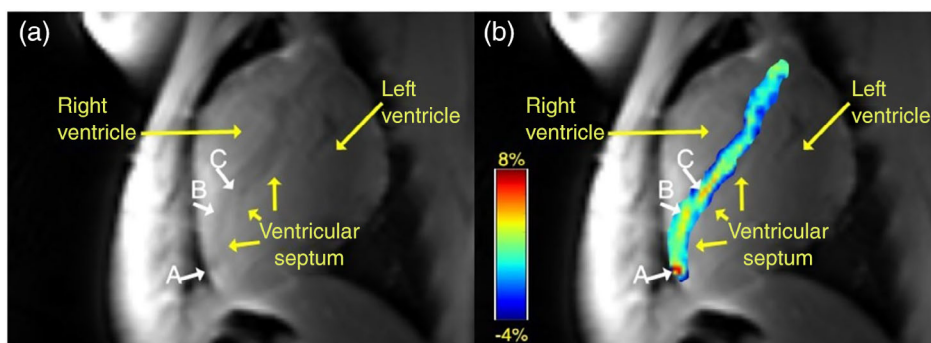


FIGURE 4 (a) An anatomical MR image of the heart showing the right ventricle, left ventricle, and the interventricular septum where the stem cells were transplanted: MSCs expressing HSV1-TK (A) and wild type MSCs (B) were incubated for 4 h with 5-MDHT prior to transplantation and control wild type MSCs (C). (b) CEST map overlaid on the anatomical image showing labeled MSC^{HSV1-TK} appearing as a hot spot (A) (Alon et al., 2016)

CEST is a nascent MRI contrast strategy based on the expression of an enzyme that triggers the exchange of a proton with surrounding water molecules from a probe that is introduced exogenously (Bar-Shir et al., 2013; Chan et al., 2013). For instance, Alon et al. successfully generated CEST contrast with MSCs transfected with herpes simplex virus type-1-thymidine kinase (HSV1-tk) in an *in vivo* myocardial infarcted pig model (Alon et al., 2016). The expression of the kinase in viable cells phosphorylates the exogenous CEST MRI probe, 5-methyl-5,6-dihydrothymidine (5-MDHT) which can then be visualized with CEST-MRI which is dependent on the exchange of amide proton on the reporter probe with the adjacent water protons. This work has demonstrated the practicality of monitoring viable MSCs by imaging gene expression with HSV1-tk via a reporter probe in an *in vivo* infarcted heart model with a 3 T MR system (Figure 4; Alon et al., 2016). However, a key issue in the clinical translation of the employment of reporter genes to track stem cells elicits safety concerns correlated with gene alteration of cells (Jurgielewicz et al., 2017). Therefore, it must be reiterated that any MRI stem cell tracking strategy should not change vital SCs properties that could have a detrimental effect on the efficacy and safety of SC treatment. Consequently, more long-term studies need to be performed to fully comprehend the safety and efficacy of MRI reporter genes in stem cell tracking for clinical translation.

While MRI presents itself as an apt imaging strategy that allows visualization and monitoring of SCs, a single modality is inadequate to obtain all essential data of implanted cells. MRI is safe for deep tissue imaging and has high resolution but low sensitivity (Sutton et al., 2008). SPIONPs have been extensively used as MR cell tracking agents due to its high sensitivity and low toxicity. However, as mentioned in this review, contrast generated by SPIO labeled cells can be mistaken with other factors due to trauma or hemorrhage (Himmelreich et al., 2005). Conversely, nuclear imaging techniques such as SPECT and PET have very high sensitivity and specificity but poor resolution (Janjic & Ahrens, 2009). Moreover, the limited half-life of tracers impedes longitudinal tracking and visualization of implanted MSCs (Belderbos et al., 2020).

Clearly, there is currently no perfect imaging strategy for the monitoring of stem cells *in vivo*. Therefore, considering the inherent limitations of current imaging modalities, we propose that the future research direction in stem cell tracking should focus on the utilization of multimodal imaging. Consequently, combining the utilization of different imaging modalities for the tracking of MSCs can overcome limitations involved with individual technique (Bhakoo, 2011). This approach encompasses the development of multifunctional contrast agents whereby complementary roles of each technique can be fully exploited. Hence, an intelligent combination to MRI would be the inclusion of clinically translatable imaging modalities such as PET, SPECT, US, and PAI.

For instance, recently, Belderbos et al demonstrated successful *in vivo* tracking of MSCs with ¹⁸F labeled Fe₃O₄@Al(OH)₃ NPs using simultaneous multimodal PET/MR imaging (Belderbos et al., 2020). Hence, PET/MR images acquired enhances visualization and quantification of labeled cells (Belderbos et al., 2020). These novel NPs displayed promising potential as a dual PET/MRI contrast agents for the longitudinal tracking of MSCs *in vivo* (Belderbos et al., 2020).

Still in infancy stage, photoacoustic imaging (PAI) is a non-invasive imaging technique which provides high contrast of optics and resolution of acoustic which allows visualizing morphological and functional characteristics (Kubelick & Emelianov, 2020). NP contrast agents are utilized to label SCs to create adequate detectable acoustic source (Kubelick & Emelianov, 2020). Hence, PAI has great potential for *in vivo* longitudinal tracking of SCs. Recently, Kubelick and Emelianov demonstrated successful utilization of tri-modal imaging with US/PAI/MRI to detect stem

cells labeled with Prussian blue nanocubes in the spinal cord of rat model (Kubelick & Emelianov, 2020). This multi-modal contrast allowed successful monitoring of SCs in the spinal cord intraoperatively and postoperatively.

5 | PROSPECTS AND CHALLENGES FOR TRANSLATION

MRI cell tracking in clinical trials is currently in its infancy stage. Till date, a few clinical studies involving SPIO based cell tracking have been reported (Callera & de Melo, 2007; de Vries et al., 2005; Toso et al., 2008; Zhu et al., 2006). In the first reported clinical study utilizing MRI cell tracking in melanoma patients, dendritic cells were labeled with SPIONs or ^{111}In -oxine and cells were co-implanted with delivery guided through ultrasound imaging, into the inguinal lymph nodes of patients (de Vries et al., 2005). This study compared the feasibility and accuracy of identifying ultrasound-guided injected cells labeled with SPIONs and radionuclide in the lymph nodes and the monitoring migration pattern of cells to distant lymph nodes using a 3 T MRI scanner and scintigraphic imaging, respectively (de Vries et al., 2005). Interestingly, labeled cells implanted via ultrasound assisted delivery were injected away from the targeted region of interest in 50% of the patients. It was found that the inaccurate injection performed by experienced radiologist was not detected using radionuclide imaging but was clearly observed using MRI (de Vries et al., 2005). Therefore, in contrast to scintigraphic imaging, MR imaging allowed evaluation of the accuracy of injected dendritic cells via ultrasound guided delivery.

Overall, this study established that MRI was capable to accurately detect cells injected in lymph nodes and was superior to radionuclide imaging in this aspect (de Vries et al., 2005). MRI-compatible catheters that allow precise MRI guided injection of cells was developed as a result of this important discovery.

A huge obstacle in this field is that pharmaceutical industries have ceased productions of SPIO agents such as ferromoxides and ferucarbotran due to lack of clinical users [128]. Presently, there are other preclinical experimental SPIO agents available with the latest clinical study recently completed involving in vivo tracking of USPIO labeled MSC in the heart (NCT03651791). This clinical study was performed to assess the feasibility of MRI tracking of labeled bone marrow derived MSCs post-intramyocardial injection in patients with chronic ischemic heart disease (Mathiasen et al., 2019). Labeled MSCs were successfully tracked with MRI for up to 14 days post-injection of cells (Figure 5; Mathiasen et al., 2019). Importantly, improved heart function was observed and labeling of MSCs with USPIO did not affect long term safety of treatment in all patients (Mathiasen et al., 2019).

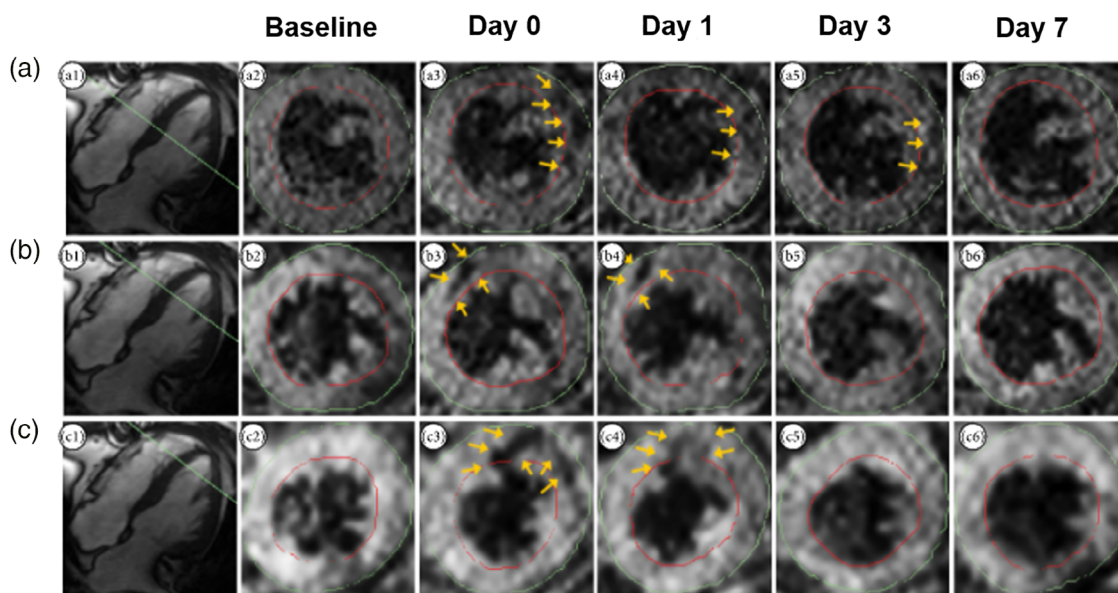


FIGURE 5 T_2^* images. T_2^* images from one representative patient. Images a1, b1, and c1 show the longitudinal position of respective short-axis images (green lines). Images a2–a6, b2–b6, and c2–c6 show serial short-axis images at the same three longitudinal positions (a, b, c) at baseline, day 0, day 1, day 3, and day 7 after injection. The yellow arrows point to hypointense areas in the images suspected to point out injected ultra-small superparamagnetic iron oxides labeled mesenchymal stem cells USPIO-labeled MSCs (slice thickness 5 mm) (Mathiasen et al., 2019)

While there are many clinical trials on the employment of MSCs in the treatment of various diseases, MRI is utilized in these studies as an imaging modality to monitor treatment efficacy and not to track implanted cells. To the best of our knowledge, only one completed clinical trial study (NCT03651791) was recorded specifically on the tracking of MSCs labeled with SPIONs in patients with chronic ischemic heart disease which was already summarized in this review (Mathiasen et al., 2019). A first-in-man, Phase I study (NCT02035085) utilizing ^{19}F MRI to track autologous, adipose derived stem cells is in recruitment phase and will only commence tentatively in December 2021. Another study (NCT03648463) involving the use of MRI labeling technique to track MSCs in orthopedic conditions was started in October 2019. However, no further updates were provided and the status for this study is classified as unknown.

Recently, there has been a channeling of focus to ^{19}F imaging for the in vivo tracking of cells which has led to the development of novel ^{19}F MRI tracers (Moonshi et al., 2018). This change is probably due to the fact that ^{19}F MRI delivers a highly specific, explicit, and quantitative strategy to monitor labeled cells in contrast to metal ion-based imaging. Immune cells labeled with PFC nanoemulsions was observed in patients with colorectal cancer in a phase 1 clinical study (NCT01671592). While this study demonstrated the feasibility of ^{19}F based cell tracking using a clinical scanner, it also underscored a huge drawback with ^{19}F imaging, which is its limited sensitivity (Boehm-Sturm et al., 2011). Only patients injected with a high quantity of (1×10^7) cells had localized detectable ^{19}F signal in comparison to a lower dose of (1×10^6) cells (Eric T. Ahrens et al., 2005). Nonetheless, from this viewpoint, a conventional MSC based clinical therapy requires more than one intravenous injection of cell quantity in the millionth range (Chambers et al., 2014; Lublin et al., 2014). Consequently, the detection sensitivity achieved here in a clinical scanner is still within the acceptable range for the purpose of cell tracking using MRI (Chambers et al., 2014; Lublin et al., 2014).

6 | CONCLUSION

Till date, MRI has not been fully exploited in the clinic for SC labeling mainly because of the lack of suitable and effective tracers. Gd-based contrast agents have not been widely employed for SC imaging due to concerns involving long term cytotoxic effects on the functional and phenotypical features of SCs. Interestingly, there have not been many published studies in the past 5 years on MR imaging with SCs labeled with SPIONs despite various reported findings highlighting successful in vivo tracking of SCs labeled with SPIONs in diseased models. Therefore, it is critical to develop reliable MR contrast agents to completely take advantage of MRI as a powerful imaging modality for the tracking of SCs. Recently, there has been a shift of direction to ^{19}F imaging for the in vivo tracking of cells which has led to the development of novel ^{19}F MRI tracers. This change in direction is likely because ^{19}F MRI delivers a highly specific, explicit, and quantitative approach to monitor labeled cells in comparison to metal ion-based imaging.

MSCs are employed as therapeutic agent or delivery vehicle in the treatment of various diseases. Hence, MRI based cell tracking has outstanding potential specifically in the optimization of parameters in SC therapy to progress toward a successful clinical translation and it is anticipated to be routinely employed in the near future. Importantly, most major hospitals are already equipped with MRI scanners, hence allowing clinical translation of SC tracking feasible. While MRI presents itself as a suitable imaging technique that allows visualization and monitoring of SCs, a single modality is insufficient to obtain all vital data of implanted cells. Therefore, combining the utilization of different imaging modalities for the tracking of MSCs can overcome shortcomings involved with individual technique.

CONFLICT OF INTEREST

The authors have declared no conflicts of interest for this article.

AUTHOR CONTRIBUTIONS

Shehzahdi Moonshi: Conceptualization (equal); writing – original draft (lead); writing – review and editing (lead). **Yuaow Wu:** Writing – review and editing (supporting). **Hang Ta:** Conceptualization (equal); funding acquisition (lead); resources (lead); supervision (lead); writing – review and editing (supporting).

DATA AVAILABILITY STATEMENT

Data sharing is not applicable to this article as no new data were created or analyzed in this study.

ORCID

Shehzahdi Shebbrin Moonshi  <https://orcid.org/0000-0003-2048-595X>

Yuao Wu  <https://orcid.org/0000-0003-4384-1195>

Hang Thu Ta  <https://orcid.org/0000-0003-1188-0472>

RELATED WIREs ARTICLES

[What is a stem cell?](#)

[Functional nanoparticles for magnetic resonance imaging](#)

REFERENCES

- Aarntzen, E. H. J. G., Srinivas, M., Radu, C. G., Punt, C. J. A., Boerman, O. C., Figdor, C. G., Oyen, W. J., & de Vries, I. J. M. (2013). In vivo imaging of therapy-induced anti-cancer immune responses in humans. *Cellular and Molecular Life Sciences: CMLS*, 70(13), 2237–2257. <https://doi.org/10.1007/s00018-012-1159-2>
- Ahrens, E. T., & Bulte, J. W. (2013). Tracking immune cells in vivo using magnetic resonance imaging. *Nature Reviews Immunology*, 13(10), 755–763. <https://doi.org/10.1038/nri3531>
- Ahrens, E. T., Flores, R., Xu, H., & Morel, P. A. (2005). In vivo imaging platform for tracking immunotherapeutic cells. *Nature Biotechnology*, 23(8), 983–987.
- Ahrens, E. T., Helfer, B. M., O'Hanlon, C. F., & Schirda, C. (2014). Clinical cell therapy imaging using a perfluorocarbon tracer and fluorine-19 MRI. *Magnetic Resonance in Medicine*, 72(6), 1696–1701. <https://doi.org/10.1002/mrm.25454>
- Alon, L., Kraitchman, D., Schär, M., Cortez, A., Yadav, N. N., Cook, J., Johnston, P., Krimins, R., McMahon, M., van Zijl, P., Bulte, J., & Gilad, A. A. (2016). Cardiac CEST-MRI for tracking stem cell survival and determining the role of CXCL2. *Journal of Cardiovascular Magnetic Resonance*, 18, P262. <https://doi.org/10.1186/1532-429X-18-S1-P262>
- Arami, H., Khandhar, A., Liggitt, D., & Krishnan, K. M. (2015). In vivo delivery, pharmacokinetics, biodistribution and toxicity of iron oxide nanoparticles. *Chemical Society Reviews*, 44(23), 8576–8607. <https://doi.org/10.1039/c5cs00541h>
- Arndt, N., Tran, H. D., Zhang, R., Xu, Z. P., & Ta, H. T. (2020). Different approaches to develop nanosensors for diagnosis of diseases. *Advanced Science*, 7(24), 2001476.
- Aspord, C., Laurin, D., Janier, M. F., Mandon, C. A., Thivolet, C., Villiers, C., Mowat, P., Madec, A. M., Tillement, O., Perriat, P., Louis, C., Bérard, F., Marche, P. N., Plumas, J., & Billotey, C. (2013). Paramagnetic nanoparticles to track and quantify in vivo immune human therapeutic cells. *Nanoscale*, 5(23), 11409–11415. <https://doi.org/10.1039/C3NR34240A>
- Bales, B. C., Grimmond, B., Johnson, B. F., Luttrell, M. T., Meyer, D. E., Polyanskaya, T., Rishel, M. J., & Roberts, J. (2019). Fe-HBED analogs: A promising class of iron-chelate contrast agents for magnetic resonance imaging. *Contrast Media & Molecular Imaging*, 2019, 8356931. <https://doi.org/10.1155/2019/8356931>
- Bar-Shir, A., Liu, G., Greenberg, M. M., Bulte, J. W. M., & Gilad, A. A. (2013). Synthesis of a probe for monitoring HSV1-tk reporter gene expression using chemical exchange saturation transfer MRI. *Nature Protocols*, 8(12), 2380–2391. <https://doi.org/10.1038/nprot.2013.140>
- Belderbos, S., González-Gómez, M. A., Cleeren, F., Wouters, J., Piñeiro, Y., Deroose, C. M., Coosemans, A., Gsell, W., Bormans, G., Rivas, J., & Himmelreich, U. (2020). Simultaneous in vivo PET/MRI using fluorine-18 labeled Fe₃O₄@Al(OH)₃ nanoparticles: Comparison of nanoparticle and nanoparticle-labeled stem cell distribution. *EJNMMI Research*, 10(1), 73. <https://doi.org/10.1186/s13550-020-00655-9>
- Bernsen, M. R., Guenoun, J., van Tiel, S. T., & Krestin, G. P. (2015). Nanoparticles and clinically applicable cell tracking. *The British Journal of Radiology*, 88(1054), 20150375. <https://doi.org/10.1259/bjr.20150375>
- Besenhart, M. O., Panariello, L., Kiefer, C., LaGrow, A. P., Storozhuk, L., Perton, F., Begin, S., Mertz, D., NTK, T., & Gavriilidis, A. (2021). Small iron oxide nanoparticles as MRI T1 contrast agent: Scalable inexpensive water-based synthesis using a flow reactor. *Nanoscale*, 13(19), 8795–8805. <https://doi.org/10.1039/D1NR00877C>
- Bhakoo, K. (2011). In vivo stem cell tracking in neurodegenerative therapies. *Expert Opinion on Biological Therapy*, 11(7), 911–920. <https://doi.org/10.1517/14712598.2011.575057>
- Bible, E., Dell'Acqua, F., Solanky, B., Balducci, A., Crapo, P. M., Badylak, S. F., Ahrens, E. T., & Modo, M. (2012). Non-invasive imaging of transplanted human neural stem cells and ECM scaffold remodeling in the stroke-damaged rat brain by (19)F- and diffusion-MRI. *Biomaterials*, 33(10), 2858–2871. <https://doi.org/10.1016/j.biomaterials.2011.12.033>
- Boehm-Sturm, P., Aswendt, M., Minassian, A., Michalk, S., Mengler, L., Adamczak, J., Mezzanotte, L., Löwik, C., & Hoehn, M. (2014). A multi-modality platform to image stem cell graft survival in the naïve and stroke-damaged mouse brain. *Biomaterials*, 35(7), 2218–2226. <https://doi.org/10.1016/j.biomaterials.2013.11.085>
- Boehm-Sturm, P., Haeckel, A., Hauptmann, R., Mueller, S., Kuhl, C. K., & Schellenberger, E. A. (2017). Low-molecular-weight iron chelates may be an alternative to gadolinium-based contrast agents for T1-weighted contrast-enhanced MR imaging. *Radiology*, 286(2), 537–546. <https://doi.org/10.1148/radiol.2017170116>
- Boehm-Sturm, P., Mengler, L., Wecker, S., Hoehn, M., & Kallur, T. (2011). In vivo tracking of human neural stem cells with 19F magnetic resonance imaging. *PLoS One*, 6(12), e29040. <https://doi.org/10.1371/journal.pone.0029040>
- Brekke, C., Morgan, S. C., Lowe, A. S., Meade, T. J., Price, J., Williams, S. C. R., & Modo, M. (2007). The in vitro effects of a bimodal contrast agent on cellular functions and relaxometry. *NMR in Biomedicine*, 20(2), 77–89. <https://doi.org/10.1002/nbm.1077>

- Bull, E., Madani, S. Y., Sheth, R., Seifalian, A., Green, M., & Seifalian, A. M. (2014). Stem cell tracking using iron oxide nanoparticles. *International Journal of Nanomedicine*, 9, 1641–1653. <https://doi.org/10.2147/IJN.S48979>
- Bulte, J. W. M., & Daldrop-Link, H. E. (2018). Clinical tracking of cell transfer and cell transplantation: Trials and tribulations. *Radiology*, 289(3), 604–615. <https://doi.org/10.1148/radiol.2018180449>
- Bulte, J. W. M., & Kraitchman, D. L. (2004). Iron oxide MR contrast agents for molecular and cellular imaging. *NMR in Biomedicine*, 17(7), 484–499. <https://doi.org/10.1002/nbm.924>
- Callera, F., & de Melo, C. M. T. P. (2007). Magnetic resonance tracking of magnetically labeled autologous bone marrow CD34+ cells transplanted into the spinal cord via lumbar puncture technique in patients with chronic spinal cord injury: CD34+ cells' migration into the injured site. *Stem Cells and Development*, 16(3), 461–466. <https://doi.org/10.1089/scd.2007.0083>
- Castro, O., Nesbitt, A. E., & Lyles, D. (1984). Effect of a perfluorocarbon emulsion (Fluosol-DA) on reticuloendothelial system clearance function. *American Journal of Hematology*, 16(1), 15–21. <https://doi.org/10.1002/ajh.2830160103>
- Chambers, D. C., Enever, D., Ilic, N., Sparks, L., Whitelaw, K., Ayres, J., Yerkovich, S. T., Khalil, D., Atkinson, K. M., & Hopkins, P. M. A. (2014). A phase 1b study of placenta-derived mesenchymal stromal cells in patients with idiopathic pulmonary fibrosis. *Respirology*, 19(7), 1013–1018. <https://doi.org/10.1111/resp.12343>
- Chan, K. W. Y., Liu, G., Song, X., Kim, H., Yu, T., Arifin, D. R., Gilad, A. A., Hanes, J., Walczak, P., van Zijl, P. C., Bulte, J. W., & McMahon, M. T. (2013). MRI-detectable pH nanosensors incorporated into hydrogels for in vivo sensing of transplanted-cell viability. *Nature Materials*, 12(3), 268–275. <https://doi.org/10.1038/nmat3525>
- Chapelin, F., Capitini, C. M., & Ahrens, E. T. (2018). Fluorine-19 MRI for detection and quantification of immune cell therapy for cancer. *Journal for Immunotherapy of Cancer*, 6(1), 105–105. <https://doi.org/10.1186/s40425-018-0416-9>
- Chapelin, F., Gao, S., Okada, H., Weber, T. G., Messer, K., & Ahrens, E. T. (2017). Fluorine-19 nuclear magnetic resonance of chimeric antigen receptor T cell biodistribution in murine cancer model. *Scientific Reports*, 7(1), 17748. <https://doi.org/10.1038/s41598-017-17669-4>
- Chapon, C., Jackson, J., Aboagye, E., Herlihy, A., Jones, W., & Bhakoo, K. (2009). An in vivo multimodal imaging study using MRI and PET of stem cell transplantation after myocardial infarction in rats. *Molecular Imaging and Biology*, 11(1), 31–38. <https://doi.org/10.1007/s11307-008-0174-z>
- Chen, P.-M., Yen, M.-L., Liu, K.-J., Sytwu, H.-K., & Yen, B.-L. (2011). Immunomodulatory properties of human adult and fetal multipotent mesenchymal stem cells. *Journal of Biomedical Science*, 18(1), 49.
- Chien, L. Y., Hsiao, J. K., Hsu, S. C., Yao, M., Lu, C. W., Liu, H. M., Chen, Y. C., Yang, C. S., & Huang, D. M. (2011). In vivo magnetic resonance imaging of cell tropism, trafficking mechanism, and therapeutic impact of human mesenchymal stem cells in a murine glioma model. *Biomaterials*, 32(12), 3275–3284. <https://doi.org/10.1016/j.biomaterials.2011.01.042>
- Clark, L. C. (1966). Survival of mammals breathing organic liquids equilibrated with oxygen at atmospheric pressure. *Science (New York, N.Y.)*, 152(3730), 1755.
- Cole, A. J., David, A. E., Wang, J., Galbán, C. J., & Yang, V. C. (2011). Magnetic brain tumor targeting and biodistribution of long-circulating PEG-modified, cross-linked starch-coated iron oxide nanoparticles. *Biomaterials*, 32(26), 6291–6301. <https://doi.org/10.1016/j.biomaterials.2011.05.024>
- Danielyan, L., Schwab, M., Siegel, G., Brawek, B., Garaschuk, O., Asavapanumas, N., Buadze, M., Lourhmati, A., Wendel, H. P., Avci-Adali, M., Krueger, M. A., Calaminus, C., Naumann, U., Winter, S., Schaeffeler, E., Spogis, A., Beer-Hammer, S., Neher, J. J., Spohn, G., ... Schäfer, R. (2020). Cell motility and migration as determinants of stem cell efficacy. *EBioMedicine*, 60, 102989. <https://doi.org/10.1016/j.ebiom.2020.102989>
- de Vries, I. J. M., Lesterhuis, W. J., Barentsz, J. O., Verdijk, P., van Krieken, J. H., Boerman, O. C., Oyen, W. J., Bonenkamp, J. J., Boezeman, J. B., Adema, G. J., Bulte, J. W., Scheenen, T. W., Punt, C. J., Heerschap, A., & Figdor, C. G. (2005). Magnetic resonance tracking of dendritic cells in melanoma patients for monitoring of cellular therapy. *Nature Biotechnology*, 23(11), 1407–1413.
- Duyn, J. (2013). MR susceptibility imaging. *Journal of Magnetic Resonance (San Diego, CA: 1997)*, 229, 198–207. <https://doi.org/10.1016/j.jmr.2012.11.013>
- Feng, Q., Liu, Y., Huang, J., Chen, K., Huang, J., & Xiao, K. (2018). Uptake, distribution, clearance, and toxicity of iron oxide nanoparticles with different sizes and coatings. *Scientific Reports*, 8(1), 2082. <https://doi.org/10.1038/s41598-018-19628-z>
- Ferrauto, G., Castelli, D. D., Terreno, E., & Aime, S. (2013). In vivo MRI visualization of different cell populations labeled with PARACEST agents. *Magnetic Resonance in Medicine*, 69(6), 1703–1711. <https://doi.org/10.1002/mrm.24411>
- Figueiredo, S., Cutrin, J. C., Rizzitelli, S., De Luca, E., Moreira, J. N., Geraldles, C. F. G. C., Aime, S., & Terreno, E. (2013). MRI tracking of macrophages labeled with glucan particles entrapping a water insoluble paramagnetic Gd-based agent. *Molecular Imaging and Biology*, 15(3), 307–315. <https://doi.org/10.1007/s11307-012-0603-x>
- Frangioni, J. V., & Hajjar, R. J. (2004). In vivo tracking of stem cells for clinical trials in cardiovascular disease. *Circulation*, 110(21), 3378–3383. <https://doi.org/10.1161/01.cir.0000149840.46523.fc>
- Frank, J. A., Miller, B. R., Arbab, A. S., Zywicke, H. A., Jordan, E. K., Lewis, B. K., Bryant, L. H., Jr., & Bulte, J. W. M. (2003). Clinically applicable labeling of mammalian and stem cells by combining superparamagnetic iron oxides and transfection agents. *Radiology*, 228(2), 480–487. <https://doi.org/10.1148/radiol.2281020638>
- Gaston, E., Fraser, J. F., Xu, Z. P., & Ta, H. T. (2018). Nano- and micro-materials in the treatment of internal bleeding and uncontrolled hemorrhage. *Nanomedicine: Nanotechnology, Biology and Medicine*, 14(2), 507–519.
- Gaudet, J. M., Hamilton, A. M., Chen, Y., Fox, M. S., & Foster, P. J. (2017). Application of dual 19F and iron cellular MRI agents to track the infiltration of immune cells to the site of a rejected stem cell transplant. *Magnetic Resonance in Medicine*, 78(2), 713–720. <https://doi.org/10.1002/mrm.26400>

- Gaudet, J. M., Ribot, E. J., Chen, Y., Gilbert, K. M., & Foster, P. J. (2015). Tracking the fate of stem cell implants with Fluorine-19 MRI. *PLoS One*, *10*(3), e0118544. <https://doi.org/10.1371/journal.pone.0118544>
- Geng, K., Yang, Z. X., Huang, D., Yi, M., Jia, Y., Yan, G., Cheng, X., & Wu, R. (2015). Tracking of mesenchymal stem cells labeled with gadolinium diethylenetriamine pentaacetic acid by 7T magnetic resonance imaging in a model of cerebral ischemia. *Molecular Medicine Reports*, *11*(2), 954–960. <https://doi.org/10.3892/mmr.2014.2805>
- Gerhardt, G. E., & Lagow, R. J. (1978). Synthesis of the perfluoropoly(ethylene glycol) ethers by direct fluorination. *The Journal of Organic Chemistry*, *43*(23), 4505–4509. <https://doi.org/10.1021/jo00417a026>
- Geyer, R. P. (1973). Fluorocarbon-polyol artificial blood substitutes. *The New England Journal of Medicine*, *289*(20), 1077–1082. <https://doi.org/10.1056/NEJM197311152892008>
- Granot, D., Nkansah, M. K., Bennewitz, M. F., Tang, K. S., Markakis, E. A., & Shapiro, E. M. (2014). Clinically viable magnetic poly(lactide-co-glycolide) particles for MRI-based cell tracking. *Magnetic Resonance in Medicine*, *71*(3), 1238–1250. <https://doi.org/10.1002/mrm.24741>
- Gubert, F., Decotelli, A. B., Bonacossa-Pereira, I., Figueiredo, F. R., Zaverucha-do-Valle, C., Tovar-Moll, F., Hoffmann, L., Urmenyi, T. P., Santiago, M. F., & Mendez-Otero, R. (2016). Intraspinal bone-marrow cell therapy at pre- and symptomatic phases in a mouse model of amyotrophic lateral sclerosis. *Stem Cell Research & Therapy*, *7*, 41–41. <https://doi.org/10.1186/s13287-016-0293-4>
- Guenoun, J., Koning, G. A., Doeswijk, G., Bosman, L., Wielopolski, P. A., Krestin, G. P., & Bernsen, M. R. (2012). Cationic Gd-DTPA liposomes for highly efficient labeling of mesenchymal stem cells and cell tracking with MRI. *Cell Transplantation*, *21*(1), 191–205. <https://doi.org/10.3727/096368911X593118>
- Heyn, C., Ronald, J. A., Mackenzie, L. T., MacDonald, I. C., Chambers, A. F., Rutt, B. K., & Foster, P. J. (2006). In vivo magnetic resonance imaging of single cells in mouse brain with optical validation. *Magnetic Resonance in Medicine*, *55*(1), 23–29. <https://doi.org/10.1002/mrm.20747>
- Himmelreich, U., Weber, R., Ramos-Cabrer, P., Wegener, S., Kandal, K., Shapiro, E. M., Koretsky, A. P., & Hoehn, M. (2005). Improved stem cell MR detectability in animal models by modification of the inhalation gas. *Molecular Imaging*, *4*(2), 104–109.
- Hmadcha, A., Martin-Montalvo, A., Gauthier, B. R., Soria, B., & Capilla-Gonzalez, V. (2020). Therapeutic potential of mesenchymal stem cells for cancer therapy. *Frontiers in Bioengineering and Biotechnology*, *8*(43). <https://doi.org/10.3389/fbioe.2020.00043>
- Jacoby, C., Temme, S., Mayenfels, F., Benoit, N., Krafft, M. P., Schubert, R., Schrader, J., & Flögel, U. (2014). Probing different perfluorocarbons for in vivo inflammation imaging by 19F MRI: Image reconstruction, biological half-lives and sensitivity. *NMR in Biomedicine*, *27*(3), 261–271. <https://doi.org/10.1002/nbm.3059>
- Janjic, J. M., & Ahrens, E. T. (2009). Fluorine-containing nanoemulsions for MRI cell tracking. *Wiley Interdisciplinary Reviews: Nanomedicine and nanobiotechnology*, *1*(5), 492–501. <https://doi.org/10.1002/wnan.35>
- Jing, X.-H., Yang, L., Duan, X.-J., Xie, B., Chen, W., Li, Z., & Tan, H.-B. (2008). In vivo MR imaging tracking of magnetic iron oxide nanoparticle labeled, engineered, autologous bone marrow mesenchymal stem cells following intra-articular injection. *Joint Bone Spine*, *75*(4), 432–438. <https://doi.org/10.1016/j.jbspin.2007.09.013>
- Jurgielewicz, P., Harmsen, S., Wei, E., Bachmann, M. H., Ting, R., & Aras, O. (2017). New imaging probes to track cell fate: Reporter genes in stem cell research. *Cellular and Molecular Life Sciences: CMLS*, *74*(24), 4455–4469. <https://doi.org/10.1007/s00018-017-2584-z>
- Kennis, B. A., Michel, K. A., Brugmann, W. B., Laureano, A., Tao, R.-H., Somanchi, S. S., Einstein, S. A., Bravo-Alegria, J. B., Maegawa, S., Wahba, A., Kiany, S., Gordon, N., Silla, L., Schellingerhout, D., Khatua, S., Zaky, W., Sandberg, D., Cooper, L., Lee, D. A., ... Gopalakrishnan, V. (2019). Monitoring of intracerebellarly-administered natural killer cells with fluorine-19 MRI. *Journal of Neuro-Oncology*, *142*(3), 395–407. <https://doi.org/10.1007/s11060-019-03091-5>
- Kim, S. J., Lewis, B., Steiner, M.-S., Bissa, U. V., Dose, C., & Frank, J. A. (2016). Superparamagnetic iron oxide nanoparticles for direct labeling of stem cells and in vivo MRI tracking. *Contrast Media & Molecular Imaging*, *11*(1), 55–64. <https://doi.org/10.1002/cmami.1658>
- Kim, T., Momin, E., Choi, J., Yuan, K., Zaidi, H., Kim, J., Park, M., Lee, N., McMahon, M. T., Quinones-Hinojosa, A., Bulte, J. W., Hyeon, T., & Gilad, A. A. (2011). Mesoporous silica-coated hollow manganese oxide nanoparticles as positive T1 contrast agents for labeling and MRI tracking of adipose-derived mesenchymal stem cells. *Journal of the American Chemical Society*, *133*(9), 2955–2961. <https://doi.org/10.1021/ja1084095>
- Klasson, A., Ahrén, M., Hellqvist, E., Söderlind, F., Rosén, A., Käll, P.-O., Uvdal, K., & Engström, M. (2008). Positive MRI contrast enhancement in THP-1 cells with Gd2O3 nanoparticles. *Contrast Media & Molecular Imaging*, *3*(3), 106–111. <https://doi.org/10.1002/cmami.236>
- Knight, J. C., Edwards, P. G., & Paisey, S. J. (2011). Fluorinated contrast agents for magnetic resonance imaging; a review of recent developments. *RSC Advances*, *1*(8), 1415–1425. <https://doi.org/10.1039/C1RA00627D>
- Kostura, L., Kraitchman, D. L., Mackay, A. M., Pittenger, M. F., & Bulte, J. W. (2004). Feridex labeling of mesenchymal stem cells inhibits chondrogenesis but not adipogenesis or osteogenesis. *NMR in Biomedicine*, *17*(7), 513–517. <https://doi.org/10.1002/nbm.925>
- Krafft, M. P. (2001). Fluorocarbons and fluorinated amphiphiles in drug delivery and biomedical research. *Advanced Drug Delivery Reviews*, *47*(2), 209–228. [https://doi.org/10.1016/S0169-409X\(01\)00107-7](https://doi.org/10.1016/S0169-409X(01)00107-7)
- Kubelick, K. P., & Emelianov, S. Y. (2020). In vivo photoacoustic guidance of stem cell injection and delivery for regenerative spinal cord therapies. *Neurophotonics*, *7*(3), 030501. <https://doi.org/10.1117/1.NPh.7.3.030501>
- Kwon, H.-J., Shim, W. H., Cho, G., Cho, H. J., Jung, H. S., Lee, C. K., Lee, Y. S., Baek, J. H., Kim, E. J., Suh, J. Y., Sung, Y. S., Woo, D. C., Kim, Y. R., & Kim, J. K. (2015). Simultaneous evaluation of vascular morphology, blood volume and transvascular permeability using SPION-based, dual-contrast MRI: Imaging optimization and feasibility test. *NMR in Biomedicine*, *28*(6), 624–632. <https://doi.org/10.1002/nbm.3293>

- Levy, M., Luciani, N., Alloyeau, D., Elgrabli, D., Deveaux, V., Pechoux, C., Chat, S., Wang, G., Vats, N., Gendron, F., Factor, C., Lotersztajn, S., Luciani, A., Wilhelm, C., & Gazeau, F. (2011). Long term in vivo biotransformation of iron oxide nanoparticles. *Biomaterials*, 32(16), 3988–3999. <https://doi.org/10.1016/j.biomaterials.2011.02.031>
- Li, M., Wang, Y., Liu, M., & Lan, X. (2018). Multimodality reporter gene imaging: Construction strategies and application. *Theranostics*, 8(11), 2954–2973. <https://doi.org/10.7150/thno.24108>
- Liu, Y., He, Z.-J., Xu, B., Wu, Q.-Z., Liu, G., Zhu, H., Zhong, Q., Deng, D. Y., Ai, H., Yue, Q., Wei, Y., Jun, S., Zhou, G., & Gong, Q.-Y. (2011). Evaluation of cell tracking effects for transplanted mesenchymal stem cells with jetPEI/Gd-DTPA complexes in animal models of hemorrhagic spinal cord injury. *Brain Research*, 1391, 24–35. <https://doi.org/10.1016/j.brainres.2011.03.032>
- Liu, Y., Wu, Y., Zhang, R., Lam, J., Ng, J. C., Xu, Z. P., Li, L., & Ta, H. T. (2019). Investigating the use of layered double hydroxide nanoparticles as carriers of metal oxides for theranostics of ROS-related diseases. *ACS Applied Biomaterials*, 2(12), 5930–5940.
- Lublin, F. D., Bowen, J. D., Huddlestone, J., Kremenichutzky, M., Carpenter, A., Corboy, J. R., Freedman, M. S., Krupp, L., Paulo, C., Hariri, R. J., & Fischkoff, S. A. (2014). Human placenta-derived cells (PDA-001) for the treatment of adults with multiple sclerosis: A randomized, placebo-controlled, multiple-dose study. *Multiple Sclerosis and Related Disorders*, 3(6), 696–704. <https://doi.org/10.1016/j.msard.2014.08.002>
- Mathiasen, A. B., Qayyum, A. A., Jørgensen, E., Helqvist, S., Ekblond, A., Ng, M., Bhakoo, K., & Kastrup, J. (2019). In vivo MRI tracking of mesenchymal stromal cells labeled with Ultrasmall paramagnetic iron oxide particles after Intramyocardial transplantation in patients with chronic ischemic heart disease. *Stem Cells International*, 2019, 2754927. <https://doi.org/10.1155/2019/2754927>
- Mesentier-Louro, L. A., Zaverucha-do-Valle, C., da Silva-Junior, A. J., Nascimento-Dos-Santos, G., Gubert, F., de Figueirêdo, A. B. P., Torres, A. L., Paredes, B. D., Teixeira, C., Tovar-Moll, F., Mendez-Otero, R., & Santiago, M. F. (2014). Distribution of mesenchymal stem cells and effects on neuronal survival and axon regeneration after optic nerve crush and cell therapy. *PLoS One*, 9(10), e110722. <https://doi.org/10.1371/journal.pone.0110722>
- Modo, M., Beech, J. S., Meade, T. J., Williams, S. C. R., & Price, J. (2009). A chronic 1 year assessment of MRI contrast agent-labelled neural stem cell transplants in stroke. *NeuroImage*, 47, T133–T142. <https://doi.org/10.1016/j.neuroimage.2008.06.017>
- Modo, M., Cash, D., Mellodew, K., Williams, S. C. R., Fraser, S. E., Meade, T. J., Price, J., & Hodges, H. (2002). Tracking transplanted stem cell migration using bifunctional, contrast agent-enhanced, magnetic resonance imaging. *NeuroImage*, 17(2), 803–811. <https://doi.org/10.1006/nimg.2002.1194>
- Moelker, A. D., Duncker, D. J., van den Bos, E. J., Kerver, W., van der Giessen, W. J., Baks, T., Duncker, D. J., & Wielopolski, P. A. (2006). Magnetic resonance imaging of haemorrhage within reperfused myocardial infarcts: Possible interference with iron oxide-labelled cell tracking? *European Heart Journal*, 27(13), 1620–1626. <https://doi.org/10.1093/eurheartj/ehl059>
- Moonshi, S. S., Zhang, C., Peng, H., Puttick, S., Rose, S., Fisk, N. M., Bhakoo, K., Stringer, B. W., Qiao, G. G., Gurr, P. A., & Whittaker, A. K. (2018). A unique 19F MRI agent for the tracking of non phagocytic cells in vivo. *Nanoscale*, 10(17), 8226–8239. <https://doi.org/10.1039/C8NR00703A>
- Ngen, E. J., Wang, L., Kato, Y., Krishnamachary, B., Zhu, W., Gandhi, N., Smith, B., Armour, M., Wong, J., Gabrielson, K., & Artemov, D. (2015). Imaging transplanted stem cells in real time using an MRI dual-contrast method. *Scientific Reports*, 5, 13628. <https://doi.org/10.1038/srep13628>
- Ohki, A., Saito, S., & Fukuchi, K. (2020). Magnetic resonance imaging of umbilical cord stem cells labeled with superparamagnetic iron oxide nanoparticles: Effects of labelling and transplantation parameters. *Scientific Reports*, 10(1), 13684. <https://doi.org/10.1038/s41598-020-70291-9>
- Papan, P., Kantapan, J., Sangthong, P., Meepowpan, P., & Dechsupa, N. (2020). Iron (III)-quercetin complex: Synthesis, physicochemical characterization, and MRI cell tracking toward potential applications in regenerative medicine. *Contrast Media & Molecular Imaging*, 2020, 8877862. <https://doi.org/10.1155/2020/8877862>
- Parivar, K., Malekvand Fard, F., Bayat, M., Alavian, S. M., & Motavaf, M. (2016). Evaluation of iron oxide nanoparticles toxicity on liver cells of BALB/c rats. *Iranian Red Crescent Medical Journal*, 18(1), e28939. <https://doi.org/10.5812/ircmj.28939>
- Park, S., Kwak, B. K., & Jung, J. (2015). Sensitivity of susceptibility-weighted imaging in detecting superparamagnetic iron oxide-labeled mesenchymal stem cells: A comparative study. *Iranian Journal of Radiology*, 12(2), e20782. <https://doi.org/10.5812/iranradiol.20782>
- Peng, H., Blakey, I., Dargaville, B., Rasoul, F., Rose, S., & Whittaker, A. K. (2009). Synthesis and evaluation of partly fluorinated block copolymers as MRI imaging agents. *Biomacromolecules*, 10(2), 374–381. <https://doi.org/10.1021/bm801136m>
- Rehman, A. U., Wu, Y., Tran, H. D., Vazquez-Prada, K., Liu, Y., Adelnia, H., Kurniawan, N. D., Anjum, M. N., Moonshi, S. S., & Ta, H. T. (2021). Silver/iron oxide nano-popcorns for imaging and therapy. *ACS Applied Biomaterials*. <https://doi.org/10.1021/acsanm.1c01571>
- Ribot, E. J., Gaudet, J. M., Chen, Y., Gilbert, K. M., & Foster, P. J. (2014). In vivo MR detection of fluorine-labeled human MSC using the bSSFP sequence. *International Journal of Nanomedicine*, 9, 1731–1739. <https://doi.org/10.2147/IJN.S59127>
- Rosenzweig, A. (2006). Cardiac cell therapy—Mixed results from mixed cells. *The New England Journal of Medicine*, 355(12), 1274–1277. <https://doi.org/10.1056/NEJMe068172>
- Ruiz-Cabello, J., Walczak, P., Kedziorek, D. A., Chacko, V. P., Schmieder, A. H., Wickline, S. A., Lanza, G. M., & Bulte, J. W. (2008). In vivo "hot spot" MR imaging of neural stem cells using fluorinated nanoparticles. *Magnetic Resonance in Medicine*, 60(6), 1506–1511. <https://doi.org/10.1002/mrm.21783>
- Shahror, R. A., Wu, C.-C., Chiang, Y.-H., & Chen, K.-Y. (2019). Tracking superparamagnetic iron oxide-labeled mesenchymal stem cells using MRI after intranasal delivery in a traumatic brain injury murine model. *JoVE*, (153), e60450. <https://doi.org/10.3791/60450>

- Shapiro, E. M., Sharer, K., Skrtic, S., & Koretsky, A. P. (2006). In vivo detection of single cells by MRI. *Magnetic Resonance in Medicine*, 55(2), 242–249. <https://doi.org/10.1002/mrm.20718>
- Sitharaman, B., Tran, L. A., Pham, Q. P., Bolskar, R. D., Muthupillai, R., Flamm, S. D., Mikos, A. G., & Wilson, L. J. (2007). Gadofullerenes as nanoscale magnetic labels for cellular MRI. *Contrast Media & Molecular Imaging*, 2(3), 139–146. <https://doi.org/10.1002/cmml.140>
- Song, M., Moon, W. K., Kim, Y., Lim, D., Song, I.-C., & Yoon, B.-W. (2007). Labeling efficacy of superparamagnetic iron oxide nanoparticles to human neural stem cells: Comparison of Ferumoxides, monocrystalline iron oxide, cross-linked iron oxide (CLIO)-NH(2) and tat-CLIO. *Korean Journal of Radiology*, 8(5), 365–371. <https://doi.org/10.3348/kjr.2007.8.5.365>
- Srinivas, M., Aarntzen, E. H. J. G., Bulte, J. W. M., Oyen, W. J., Heerschap, A., de Vries, I. J. M., & Figdor, C. G. (2010). Imaging of cellular therapies. *Advanced Drug Delivery Reviews*, 62(11), 1080–1093. <https://doi.org/10.1016/j.addr.2010.08.009>
- Srinivas, M., Boehm-Sturm, P., Figdor, C. G., de Vries, I. J., & Hoehn, M. (2012). Labeling cells for in vivo tracking using 19F MRI. *Biomaterials*, 33(34), 8830–8840. <https://doi.org/10.1016/j.biomaterials.2012.08.048>
- Srinivas, M., Heerschap, A., Ahrens, E. T., Figdor, C. G., & de Vries, I. J. (2010). (19)F MRI for quantitative in vivo cell tracking. *Trends Biotechnol.*, 28(7), 363–370. <https://doi.org/10.1016/j.tibtech.2010.04.002>
- Srinivas, M., Morel, P. A., Ernst, L. A., Laidlaw, D. H., & Ahrens, E. T. (2007). Fluorine-19 MRI for visualization and quantification of cell migration in a diabetes model. *Magnetic Resonance in Medicine*, 58(4), 725–734. <https://doi.org/10.1002/mrm.21352>
- Srivastava, A. K., & Bulte, J. W. M. (2014). Seeing stem cells at work in vivo. *Stem cell reviews*, 10(1), 127–144. <https://doi.org/10.1007/s12015-013-9468-x>
- Sterenczak, K. A., Meier, M., Glage, S., Meyer, M., Willenbrock, S., Wefstaedt, P., Dorsch, M., Bullerdiek, J., Murua Escobar, H., Hedrich, H., & Nolte, I. (2012). Longitudinal MRI contrast enhanced monitoring of early tumour development with manganese chloride (MnCl₂) and superparamagnetic iron oxide nanoparticles (SPIOs) in a CT1258 based in vivo model of prostate cancer. *BMC Cancer*, 12, 284–284. <https://doi.org/10.1186/1471-2407-12-284>
- Sutton, E. J., Henning, T. D., Pichler, B. J., Bremer, C., & Daldrup-Link, H. E. (2008). Cell tracking with optical imaging. *European Radiology*, 18(10), 2021–2032. <https://doi.org/10.1007/s00330-008-0984-z>
- Ta, H., Prabhu, S., Leitner, E., Putnam, K., Jia, F., Bassler, N., Peter, K., & Hagemeyer, C. (2010). A novel biotechnological approach for targeted regenerative cell therapy and molecular imaging of atherothrombosis. *Heart, Lung and Circulation*, 19, S10.
- Ta, H. T., Li, Z., Hagemeyer, C., Wu, Y., Lim, H. J., Wang, W., Wei, J., Cowin, G., Whittaker, A., & Peter, K. (2018). Novel biotechnological solutions based on metal oxide and metal to preserve and assess organs for transplantation. *Cryobiology*, 81, 233.
- Taylor, A., Sharkey, J., Plagge, A., Wilm, B., & Murray, P. (2018). Multicolour in vivo bioluminescence imaging using a NanoLuc-based BRET reporter in combination with firefly luciferase. *Contrast Media & Molecular Imaging*, 2018, 2514796. <https://doi.org/10.1155/2018/2514796>
- Taylor, P. (1998). Ostwald ripening in emulsions. *Advances in Colloid and Interface Science*, 75(2), 107–163. [https://doi.org/10.1016/S0001-8686\(98\)00035-9](https://doi.org/10.1016/S0001-8686(98)00035-9)
- Thurecht, K. J. (2012). Polymers as probes for multimodal imaging with MRI. *Macromolecular Chemistry and Physics*, 213(24), 2567–2572. <https://doi.org/10.1002/macp.201200420>
- Tirotta, I., Dichiarante, V., Pigliacelli, C., Cavallo, G., Terraneo, G., Bombelli, F. B., Metrangolo, P., & Resnati, G. (2015). 19F magnetic resonance imaging (MRI): From design of materials to clinical applications. *Chemical Reviews*, 115(2), 1106–1129. <https://doi.org/10.1021/cr500286d>
- Toso, C., Vallee, J. P., Morel, P., Ris, F., Demuylder-Mischler, S., Lepetit-Coiffe, M., Marangon, N., Saudek, F., James Shapiro, A. M., Bosco, D., & Berney, T. (2008). Clinical magnetic resonance imaging of pancreatic islet grafts after iron nanoparticle labeling. *American Journal of Transplantation*, 8(3), 701–706. <https://doi.org/10.1111/j.1600-6143.2007.02120.x>
- Tran, L. A., Hernández-Rivera, M., Berlin, A. N., Zheng, Y., Sampaio, L., Bové, C., Cabreira-Hansen Mda, G., Willerson, J. T., Perin, E. C., & Wilson, L. J. (2014). The use of gadolinium-carbon nanostructures to magnetically enhance stem cell retention for cellular cardiomyoplasty. *Biomaterials*, 35(2), 720–726. <https://doi.org/10.1016/j.biomaterials.2013.10.013>
- Tseng, C.-L., Shih, I. L., Stobinski, L., & Lin, F.-H. (2010). Gadolinium hexanedione nanoparticles for stem cell labeling and tracking via magnetic resonance imaging. *Biomaterials*, 31(20), 5427–5435. <https://doi.org/10.1016/j.biomaterials.2010.03.049>
- Vande Velde, G., Himmelreich, U., & Neeman, M. (2013). Reporter gene approaches for mapping cell fate decisions by MRI: Promises and pitfalls. *Contrast Media & Molecular Imaging*, 8(6), 424–431. <https://doi.org/10.1002/cmml.1590>
- Vazquez-Prada, K. X., Lam, J., Kamato, D., Ping Xu, Z., Little, P. J., & Ta, H. T. (2020). Targeted molecular imaging of cardiovascular diseases by iron oxide nanoparticles. *Arteriosclerosis, Thrombosis, and Vascular Biology*, 41(2), 601–613.
- Wang, S., Qu, X., & Zhao, R. (2012). Clinical applications of mesenchymal stem cells. *Journal of Hematology & Oncology*, 5(1), 19.
- Wang, Y.-X. J. (2015). Current status of superparamagnetic iron oxide contrast agents for liver magnetic resonance imaging. *World Journal of Gastroenterology*, 21(47), 13400–13402. <https://doi.org/10.3748/wjg.v21.i47.13400>
- Wang, Y., Xu, C., & Ow, H. (2013). Commercial nanoparticles for stem cell labeling and tracking. *Theranostics*, 3(8), 544–560. <https://doi.org/10.7150/thno.5634>
- Wang, Y. X. J., Wang, H. H., Au, D. W. T., Zou, B. S., & Teng, L. S. (2008). Pitfalls in employing superparamagnetic iron oxide particles for stem cell labelling and in vivo MRI tracking. *The British Journal of Radiology*, 81(972), 987–988. <https://doi.org/10.1259/bjr/55991430>
- Wu, Y., Vazquez-Prada, K. X., Liu, Y., Whittaker, A. K., Zhang, R., & Ta, H. T. (2021). Recent advances in the development of theranostic nanoparticles for cardiovascular diseases. *Nanotheranostics*, 5(4), 499.

- Wu, Y., Zhang, R., Tran, H. D., Kurniawan, N. D., Moonshi, S. S., Whittaker, A. K., & Ta, H. T. (2021). Chitosan Nanococktails containing both ceria and superparamagnetic iron oxide nanoparticles for reactive oxygen species-related theranostics. *ACS Applied Nano Materials*, 4(4), 3604–3618.
- Wydra, R. J., Oliver, C. E., Anderson, K. W., Dziubla, T. D., & Hilt, J. Z. (2015). Accelerated generation of free radicals by iron oxide nanoparticles in the presence of an alternating magnetic field. *RSC Advances*, 5(24), 18888–18893. <https://doi.org/10.1039/C4RA13564D>
- Yang, Y., Pang, M., Du, C., Liu, Z.-Y., Chen, Z.-H., Wang, N.-X., Zhang, L. M., Chen, Y. Y., Mo, J., Dong, J. W., Xie, P. G., Wang, Q. Y., Liu, B., & Rong, L.-M. (2021). Repeated subarachnoid administrations of allogeneic human umbilical cord mesenchymal stem cells for spinal cord injury: A phase 1/2 pilot study. *Cytotherapy*, 23(1), 57–64. <https://doi.org/10.1016/j.jcyt.2020.09.012>
- Yu, Y. B. (2013). Fluorinated dendrimers as imaging agents for ¹⁹F MRI. *Wiley Interdisciplinary Reviews: Nanomedicine and Nanobiotechnology*, 5(6), 646–661. <https://doi.org/10.1002/wnan.1239>
- Yusof, N. N. M., McCann, A., Little, P. J., & Ta, H. T. (2019). Non-invasive imaging techniques for the differentiation of acute and chronic thrombosis. *Thrombosis Research*, 177, 161–171.
- Zhang, Z., Bos, E. J. V. D., Wielopolski, P. A., Jong-Popijus, M. D., Bernsen, M. R., Duncker, D. J., & Krestin, G. P. (2005). In vitro imaging of single living human umbilical vein endothelial cells with a clinical 3.0-T MRI scanner. *Magnetic Resonance Materials in Physics, Biology, and Medicine*, 18(4), 175–185. <https://doi.org/10.1007/s10334-005-0108-6>
- Zhu, J., Zhou, L., & XingWu, F. (2006). Tracking neural stem cells in patients with brain trauma. *New England Journal of Medicine*, 355(22), 2376–2378. <https://doi.org/10.1056/NEJMc055304>
- Zia, A., Wu, Y., Nguyen, T., Wang, X., Peter, K., & Ta, H. T. (2020). The choice of targets and ligands for site-specific delivery of nanomedicine to atherosclerosis. *Cardiovascular Research*, 116(13), 2055–2068.

How to cite this article: Moonshi, S. S., Wu, Y., & Ta, H. T. (2021). Visualizing stem cells in vivo using magnetic resonance imaging. *Wiley Interdisciplinary Reviews: Nanomedicine and Nanobiotechnology*, e1760. <https://doi.org/10.1002/wnan.1760>